

University of Reading
School of Mathematics, Meteorology and Physics

**Evaluation of Fractional Dispersion
Models**

by

Rachel Pritchard

August 2008

This dissertation is submitted to the Department of Mathematics and
Meteorology in partial fulfilment of the requirements for the degree of Master of
Science

Abstract

The usual second order advection-diffusion equation is known to under predict dispersion in turbulent flows. It is thought we can replace the diffusion term with a fractional diffusion term to better predict the dispersion.

The main concern of this work will be the numerical methods used for solving the fractional diffusion equation. Before we are able to begin with the derivation of the numerical schemes, an understanding of some fractional calculus is needed, we will therefore give a discussion on this and detail the definitions and derivatives which are needed for our numerical methods.

We notice in the literature that it is mainly finite difference methods that have been proposed. We shall see that this is perhaps the most obvious and straight forward numerical method to develop given the definitions for fractional derivatives. Due to the non-local nature of the fractional derivative the finite difference approach is computationally expensive as it usually requires a large number of degrees of freedom to obtain an accurate solution. We will therefore be interested in developing other numerical schemes in particular schemes based on non-local methods such as the spectral method.

Acknowledgments

I would like to acknowledge my supervisor Emmanuel Hanert for his help and guidance with this project. I would also like to acknowledge my mum for proof reading a draft. And finally I would like to acknowledge the financial support of the Natural Environmental Research Council (NERC) for the Masters programme 2007-08. Also a big thank you to my fellow master students who have provided some valuable comic entertainment over the year.

Declaration

I confirm that this is my own work and the use of all material from other sources has been properly and fully acknowledged.

Contents

1	Introduction	1
1.1	Why Fractional Dispersion	1
1.2	Areas Fractional Diffusion is Used	2
2	Ordinary Diffusion and Fractional Diffusion	4
2.1	Diffusion	4
2.2	Brownian Motion	6
2.3	Lévy Motion	8
2.4	Fractional Fick's Law	10
2.5	Comparison between Brownian and Lévy Motions	11
3	Fractional Calculus	13
3.1	Main Definition	13
3.2	Other Definitions	15
3.3	Standard Derivatives	17
3.4	Binomial Coefficients and Gamma Functions	19
4	Finite Difference Approximations	23
4.1	Numerical Approximation	23

4.2	A 1D Test Case	26
4.2.1	Left Scheme Test	26
4.2.2	Right Scheme Test	27
4.2.3	Accuracy of the Schemes	28
4.2.4	Stability	29
4.3	A 2D Test Case	30
4.3.1	Test of 2D Scheme	31
4.3.2	Accuracy	33
4.4	The 1D Central Scheme Results	33
4.5	Two Dimensional Results	37
4.6	A 2D Advection Diffusion Plume	40
5	A numerical scheme using Spectral Methods	43
5.1	A spectral method for fractional diffusion	44
5.2	Choices of expansion function	46
5.2.1	Cosine Expansion Function	47
5.2.2	Sine Expansion Function	48
5.2.3	Complex Exponential Expansion Function	49
5.3	Results and Comparison with Finite Difference Scheme	51
6	Conclusions and Future Work	55
6.1	Fractional Diffusion	55
6.2	Finite Difference Method	56
6.3	Spectral Method	57
	Bibliography	57

Chapter 1

Introduction

1.1 Why Fractional Dispersion

The second order advection-dispersion equation is usually used to model dispersion in flows. However in complex flows such as turbulent flows this model is no longer adequate, in fact it under predicts dispersion.

In non turbulent flows the dispersion of a contaminant is driven by the mean flow velocity and local interactions between particles i.e. particles push each other. This results in a series of small amplitude, random displacements of the contaminant particles and is known as Brownian motion. However, in complex flows such as flow through porous medium or turbulent flows it is now possible to have large variations from the mean velocity in the flow. This results in particles of the contaminant being dispersed large distances in the flow. Brownian motion is no longer an adequate description for this type of dispersion, we wish to model a type of motion that allows the large scale transport of the contaminant particles in complex flows.

A proposed way of modelling this type of dispersion is to use Lévy motion. The probability distribution function (PDF) of Lévy motion is known as Lévy distri-

butions. Unlike the Gaussian distribution, which is the PDF of Brownian motion, Lévy distributions have heavier tails and an infinite variance which implies they allow contaminant particles to be dispersed or jump large distances. Where the second order advection-dispersion equation is describing Brownian motion, Lévy motion can be described by a fractional order advection-diffusion equation. Therefore we wish to use the fractional advection-diffusion equation to model dispersion in these complex flows, with the purpose that this will give us a more realistic model of the dispersion.

The fractional advection-dispersion equation only uses a fractional derivative on the diffusion term therefore it is the diffusion term that will be made the focus of this work. We will discuss in more detail why the regular theory for diffusion falls short for describing diffusion in turbulent flows and then propose the fractional model and why it is better suited to this situation.

1.2 Areas Fractional Diffusion is Used

'According to M.Meerschaert [8] the theory behind fractional calculus is nearly as old as that for regular calculus'. 'The Fractional Calculus by Oldham and Spanier [12] states that Liouville proposed a definition in the form of expanded functions in a series of exponentials in 1832. Later in 1853 Reimann proposed a definition involving definite integrals. It was Grunwald in 1867 who unified the Riemann and Liouville definitions'. The most recent developments using fractional calculus have been using fractional derivatives in differential equations which can then be used to model many physical situations some of which we shall now discuss.

There are various areas in which the fractional derivative has been used to predict diffusion these include particle diffusion in gravel bed flows, water transport in unsaturated soils and anomalous diffusion where diffusion occurs at a different rate to the regular Gaussian diffusion. Meltzler and Sornette [11, 14] discuss a variety of these uses in physics, biology and geology. There are also financial applications

which take into account extreme market volatility. Here instead of modelling particle jumps price jumps are modelled see [8].

One example from [14] talks about anomalous diffusion in fluids which are partitioned into convective cells e.g a steady state atmosphere. Diffusion here is characterised by two types of motion, one is the fast convective motion within a convective cell and the other is the random walk behaviour for the crossing of the convective cells, this type of motion leads to the diffusion behaviour at large scales.

There are also many papers on diffusion through porous media in aquifers see [2, 13] the ideas developed in this area will be of particular use to us. A specific example of this is given by Benson [2] it details the dispersion of a contaminant in the Cape Cod Aquifer. Here a tracer was introduced into a sand and gravel aquifer and the fractional advection-dispersion equation was used to try and model the flow of this tracer.

The fractional derivative can also be used on the time derivative instead of the space derivative, here the fractional value would be between 0 and 1. 'Lin and Xu [7] state that taking the time derivative to be fractional acts as a memory of previous states of the solution as the solution at many previous time steps is required in getting the next'. Developed in their paper are the numerical methods for solving this sort of equation.

However, the area of most interest to us is using the fractional diffusion equation to predict the diffusion of a contaminant in turbulent flows. Examples include the diffusion of moisture or pollutants in the atmosphere, salinity or contaminants in the ocean and even the dispersion of sediments or contaminants in rivers and lakes.

Chapter 2

Ordinary Diffusion and Fractional Diffusion

Before we begin constructing a numerical scheme we want to understand the principles behind fractional diffusion. It is perhaps easiest to begin by looking at ordinary diffusion. This will also help us determine why this theory can be improved upon when predicting diffusion in turbulent flows and why the fractional approach is a reasonable one to take.

2.1 Diffusion

To describe the process of diffusion consider a quantity of a fluid split into two volumes which lie next to each other, one volume has a high concentration of a contaminant and the other a low concentration, see Fig. 2.1. 'According to Crank [4] molecules move randomly and have no preferred direction of motion to either volume of higher or lower concentration. However we still get a mixing because we can say that a fraction of the molecules in the volume of lower concentration will move to the higher concentration and the same fraction will move from the higher concentration to the lower concentration. Hence a net movement of molecules from high concentration to low concentration'.

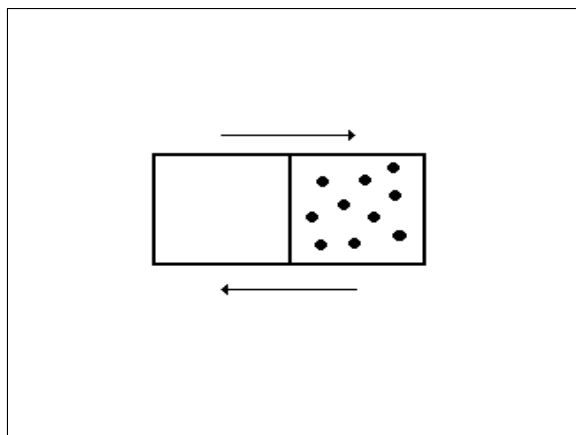


Figure 2.1: Particles diffusing between two volumes

This idea leads us to Fick's Law,

$$F = -K \frac{\partial c}{\partial x}, \quad (2.1)$$

which states that the particle flux is proportional to the concentration gradient acting towards the area of lower concentration [4]. The diffusion equation can then be obtained by taking changes of the concentration in the volume with respect to time, this is equal to the negative of the rate of change of the flux from the volume giving,

$$\frac{\partial c}{\partial t} = -\frac{\partial F}{\partial x} = \frac{\partial}{\partial x} \left(K \frac{\partial c}{\partial x} \right). \quad (2.2)$$

The diffusion equation. K is known as the diffusion coefficient.

It is important to see that Fick's law is a local process, Fig. 2.1, particles are only transported to other volumes next to their current volume in the flow, which is caused by the gradient of the concentration between the two volumes. 'Again from Crank [4] it is stated that Fick's law is only consistent for an isotropic medium which is a flow in which its structure and diffusion properties are the same in the

neighbourhood of any point'. This presents a problem when considering diffusion in turbulent flows.

In turbulent flows diffusion is due to the random fluctuations in the velocity, this can randomly transport particles of the contaminant over larger distances i.e beyond the local volumes. This is easy to imagine if we consider the analogy of rotating eddies in a flow, here the velocities in the flow varies greatly. Therefore we want a method for modelling diffusion that provides a more global process. [13] provides a discussion on this for the case where velocity variations are produced by flow through porous medium rather than eddies. To develop this new method of modelling diffusion we first need to look at Brownian motion which will lead us on to Lévy motion and the global process.

2.2 Brownian Motion

To introduce the idea of Brownian motion we first find the solution of the second order diffusion Eq. (2.2) using Fourier transforms, see [8]. To do this we take Fourier transforms in Eq. (2.2) where the Fourier transform of $c(x, t)$ is,

$$\hat{c}(k, t) = \int_{-\infty}^{\infty} e^{-ikx} c(x, t) dx.$$

This gives us the ordinary differential equation,

$$\frac{d\hat{c}(k, t)}{dt} = (ik)^2 \hat{c}(k, t) = -k^2 \hat{c}(k, t).$$

The ordinary differential equation can then be solved to give,

$$\hat{c}(k, t) = e^{-k^2 t},$$

which inverts to a Gaussian distribution.

'Brownian motion has the probability density function (PDF) of a Gaussian dis-

tribution, this can be worked out by letting X_n be a particle jump at time n and letting $S_n = X_1 + \dots + X_n$ be the location of a particle at time n , [8]'. We then apply DeMoivre's central limit theorem (CLT) see [13],

$$\lim_{n \rightarrow \infty} \frac{S_n - n\mu}{\sigma n^{\frac{1}{2}}} = N(\mu = 0, \sigma^2 = 1)$$

where σ gives the standard deviation and μ gives the mean value. The central limit theorem states that this sum of independently identically distributed (IID) variables divided by the \sqrt{n} will converge to a normal distribution, a Gaussian distribution with zero mean and variance one. It is important to note here that the CLT has a finite variance, so particles in Brownian motion move in short random motions.

Since we get a Gaussian distribution for the Fourier transform solution of the second order diffusion equation and as the limiting PDF of Brownian motion we can say that the concentration of a contaminant in a cloud of diffusing particles described by Brownian motion is a solution to the second order diffusion equation.

Fig. 2.2 gives a picture of Brownian motion and the limiting Gaussian distribution. The Gaussian distribution figure shows that the probability of larger displacements in particles tails off to zero at the edges of the distribution. If we want to model a process that favours larger displacements we need our model to have a PDF that has thicker tails, i.e. a greater probability of larger displacements.

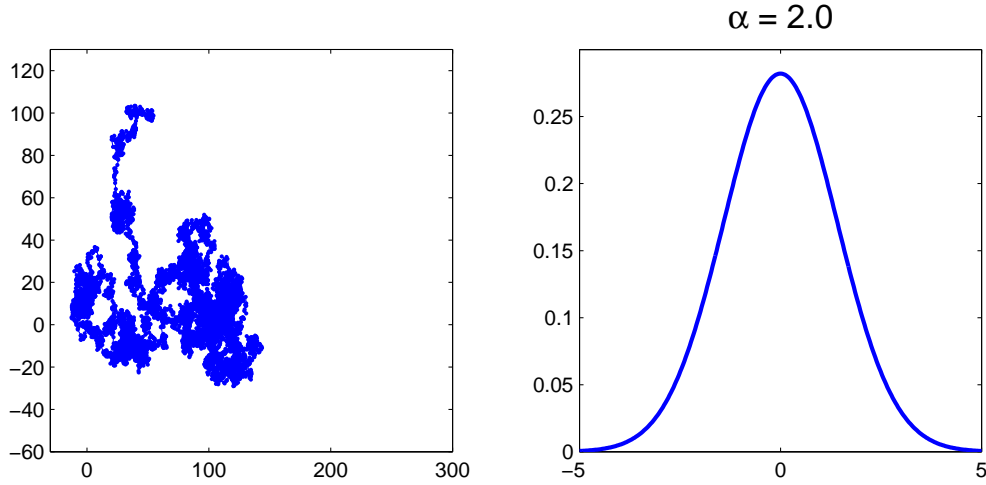


Figure 2.2: Brownian motion and Gaussian distribution

2.3 Lévy Motion

It is thought that a better representation for turbulent flows is Lévy motion, we can see from Fig. 2.3 that its path has a larger spread. Like Brownian motion can be represented by a Gaussian distribution, Lévy motion can also be represented by a PDF known as Lévy distributions this can also be seen in Fig. 2.3.

The Lévy distributions are the PDF that we use to improve our diffusion model, we are basically just replacing the Gaussian distribution by the Lévy distribution. Lévy distributions have thicker tails than the Gaussian distribution. Schummer et.al. [13] describes how they can be obtained by using a general limit theorem (GLT),

$$\lim_{n \rightarrow \infty} \frac{S_n - n\mu}{\sigma n^{\frac{1}{\alpha}}} = S_{\alpha}(\sigma = 1, \beta, \mu = 0).$$

The central limit theorem is a special case of this. The general limit theorem states that the sum of IID will converge to a "Lévy-stable" distribution, $0 < \alpha \leq 2$ is the index of stability, $-1 \leq \beta \leq 1$ the skewness coefficient, $\mu = 0$ the shift parameter and $\sigma = 1$ the spread parameter. Here σ is no longer the standard deviation since Lévy motion has an infinite variance, instead it measures the size of the spread

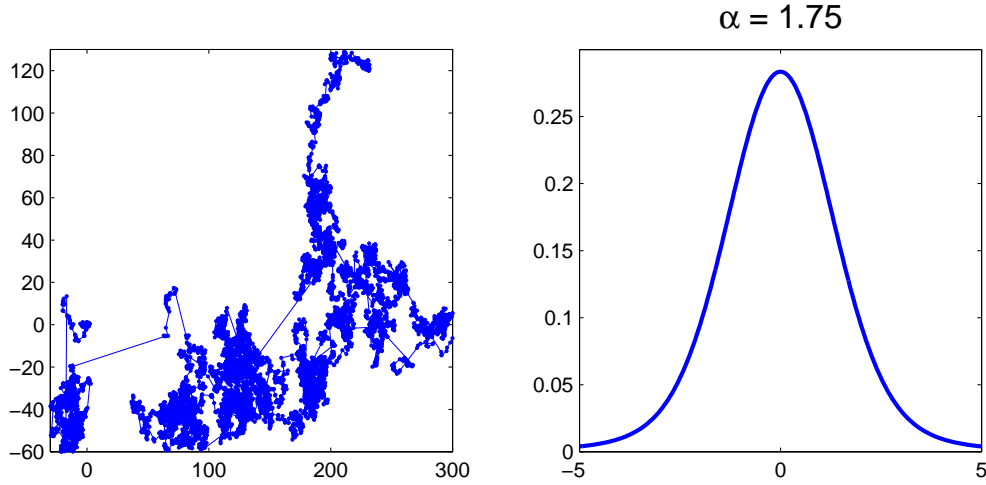


Figure 2.3: Levy motion and Levy distribution

of the distribution. Having infinite variance allows larger random movements of particles than those in Brownian motion.

The Lévy stable distributions, are expressed in terms of their Fourier transforms since they cannot all be expressed in closed form [13],

$$\int_{-\infty}^{\infty} e^{ikx} f(x) dx = \exp \left(-\sigma^\alpha |k|^\alpha \left(1 - i\beta(\text{sign}(k)) \tan \frac{\pi\alpha}{2} \right) + i\mu k \right)$$

if $\alpha \neq 1$, where $f(x)$ is a stable density and

$$\text{sign}(k) = \begin{cases} 1 & \text{if } k > 0 \\ -1 & \text{if } k < 0. \end{cases}$$

These Lévy distributions are also a solution to the fractional diffusion equation. Sornette [14] shows this for the advection-diffusion equation we shall adapt it just the diffusion equation by ignoring the advection term. Sornette first proceeds by splitting the diffusion term into the plus and minus derivatives this gives our

equation as,

$$\frac{\partial c(x, t)}{\partial t} = Bq \frac{\partial^\alpha c(x, t)}{\partial(-x)^\alpha} + Bp \frac{\partial^\alpha c(x, t)}{\partial x^\alpha}$$

if we then take fourier transforms we obtain the solution,

$$\hat{c}(k, t) = \exp [Btq(-ik)^\alpha + Btp(ik)^\alpha].$$

Then using,

$$(ik)^\alpha = (e^{\frac{i\pi}{2}} k)^\alpha = |k|^\alpha \cos \frac{\pi\alpha}{2} \left\{ 1 + i \text{sign}(k) \tan \frac{\pi\alpha}{2} \right\},$$

we get the solution as,

$$\hat{c}(k, t) = \exp \left[Bt|k|^\alpha \cos \frac{\pi\alpha}{2} \left\{ 1 + i\beta \text{sign}(k) \tan \frac{\pi\alpha}{2} \right\} \right],$$

with skewness $\beta = p - q$ and the spread parameter $\sigma^\alpha = -Bt \cos \frac{\pi\alpha}{2}$. This is a Lévy stable distribution and hence the fractional diffusion is describing Lévy motion.

2.4 Fractional Fick's Law

We can obtain the fractional diffusion equation from a fractional ficks law.

$$F = -K_\alpha \frac{\partial^q c}{\partial x^q} \tag{2.3}$$

with $\alpha = q + 1$.

It is thought that Fig. 2.4 corresponds to a fractional ficks law, which illustrates the movement of particles to volumes further away than the immediate vicinity. In a similar way to obtaining the second order diffusion equation and taking the diffusion coefficient as constant we can then get the fractional order diffusion equation as,

$$\frac{\partial c}{\partial t} = K_\alpha \frac{\partial^\alpha c}{\partial x^\alpha}. \tag{2.4}$$

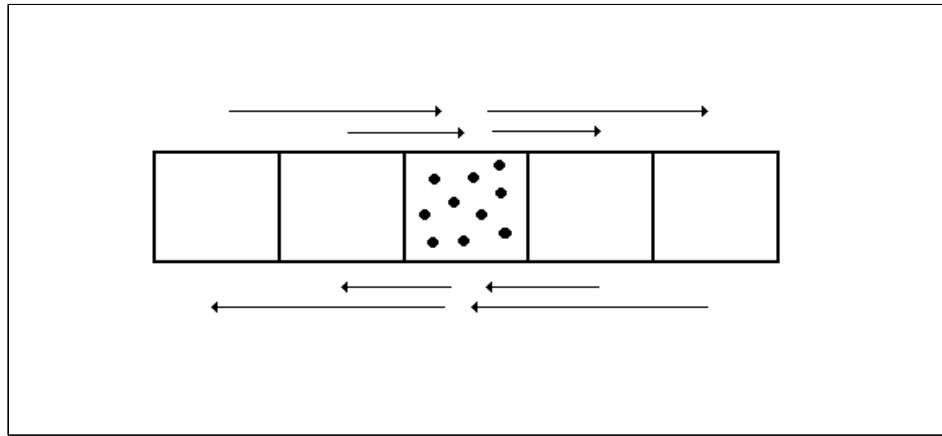


Figure 2.4: Diffusion allowed by a Fractional Fick's law

This is a non-local process the reasoning for this can clearly be seen from the definitions of the fractional derivative which involves a sum of values over the entire domain, the details of this will be introduced later.

2.5 Comparison between Brownian and Lévy Motions

Comparing the Lévy distribution to the Gaussian distribution we see that the Lévy distribution has thicker tails. The thickness of the tails depends on the value for α , as α decreases the thickness of the tail increases. This means that there will be a higher probability of larger displacements than for the Gaussian distribution. In a turbulent flow we would expect particles to be more likely to move further than in a uniform flow.

According to Meerschaert [8], for Brownian motion a cloud of diffusing particles spreads at a rate of $t^{\frac{1}{2}}$ and for Lévy motion a cloud of diffusing particles spreads at a rate of $t^{\frac{1}{\alpha}}$. This is illustrated in Fig. 2.5, in which we can see that the lower

the value of α the faster the overall diffusion, however to begin with the fractional diffusion spreads slower.

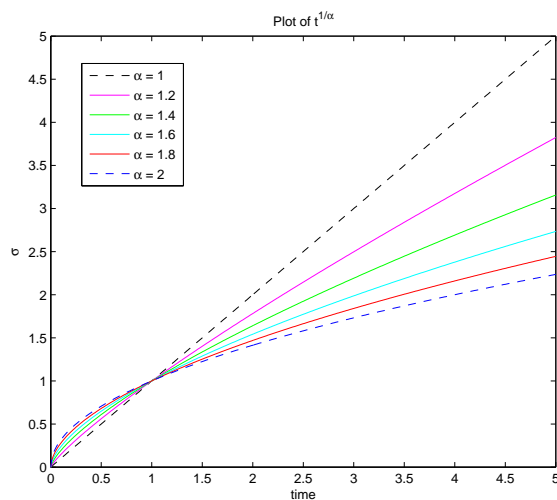


Figure 2.5: Rate of spread of a cloud of diffusing particles

In Fig. 2.5 $K_\alpha = 1$ for every value of α . The value of K_α is difficult to determine as its units alter depending on the value of α , K_α has units $\text{distance}^\alpha/\text{time}$,

$$[K_\alpha] = \frac{L^\alpha}{T}.$$

Because of these different units the suitability of a direct comparison of results using different α is something to think about. One idea to take the dimensionless diffusion equation and then say how the K_α relate to one another. For the purpose of this work we will only be concerned with taking $K_\alpha = 1$ and looking at the results produced.

Chapter 3

Fractional Calculus

Before we begin to develop any sort of numerical scheme we need to become familiar with fractional derivatives and how they are defined. If we consult [12] we see that there are many definitions for the fractional derivative and ways of defining the derivatives of standard functions.

3.1 Main Definition

Perhaps the easiest way to see where one of these definitions comes from is to first look at the limit definition for ordinary differentiation,

$$\frac{d^n f}{dx^n} \equiv \lim_{\Delta x \rightarrow 0} \frac{1}{\Delta x^n} \left(\sum_{k=0}^n (-1)^k \binom{n}{k} f(x - k\Delta x) \right). \quad (3.1)$$

Here n and k are integers. For the fractional derivative we want to change n from an integer to a real number, called α . This creates a problem in Eq. (3.1) since the binomial coefficient,

$$(-1)^k \binom{\alpha}{k}$$

is not defined for real values. To deal with this we use the following identity, as given in [12]:

$$(-1)^k \binom{\alpha}{k} = \frac{\Gamma(k - \alpha)}{\Gamma(-\alpha)\Gamma(k + 1)}.$$

Another problem is that we cannot sum up to a fractional value so instead we sum up to infinity, this is valid as the use of Gamma functions will allow results for high values of k . This arrangement of Gamma functions will later be referred to as a weight.

All this gives us our definition for the fractional derivative as

$$\frac{d^\alpha f}{dx^\alpha} \equiv \lim_{\Delta x \rightarrow 0} \frac{1}{\Delta x^\alpha} \left(\sum_{k=0}^{\infty} \frac{\Gamma(k - \alpha)}{\Gamma(-\alpha)\Gamma(k + 1)} f(x - k\Delta x) \right). \quad (3.2)$$

This is known as the Grunwald derivative and is valid over $-\infty$ to x . For a definition valid over x to ∞ we use the forward difference definition instead of the backwards difference definition resulting in the following

$$\frac{d^\alpha f}{d(-x)^\alpha} \equiv \lim_{\Delta x \rightarrow 0} \frac{1}{\Delta x^\alpha} \left(\sum_{k=0}^{\infty} \frac{\Gamma(k - \alpha)}{\Gamma(-\alpha)\Gamma(k + 1)} f(x + k\Delta x) \right). \quad (3.3)$$

These definitions will encourage more of a left diffusion for Eq. (3.2) or a right diffusion for Eq. (3.3). Numerical methods described by Meerschaert, Tadjeran and Scheffler [10, 9, 15] just use the left sided definition and give details of stability regions of the various methods and a comparison to an analytical result. However, what is really needed is a central definition which takes its values over $-\infty$ to ∞ , this definition is given by Schumer et.al. [13], it uses both the above definitions combining them to give,

$$D_\beta^\alpha = \left[\frac{1}{2}(1 - \beta)\right] D_+^\alpha + \left[\frac{1}{2}(1 + \beta)\right] D_-^\alpha. \quad (3.4)$$

Here we are using the notation,

$$D_-^\alpha = \frac{d^\alpha c}{d(-x)^\alpha}$$

and

$$D_+^\alpha = \frac{d^\alpha c}{dx^\alpha}.$$

$\frac{1}{2}(1-\beta)$ and $\frac{1}{2}(1+\beta)$ gives the probability of whether a particle will jump backwards or forwards respectively, with $-1 \leq \beta \leq 1$. The use of the β value allows us to select whether a particle will diffuse more to the left or to the right. If $\beta = 1$ we just get Eq. (3.2) and if $\beta = -1$ we just get Eq. (3.3). We can see from these definitions that the fractional derivative uses a sum of all values over the domain. The amount of dependence on each grid point is determined by the value of the Gamma functions, what we call the weight.

3.2 Other Definitions

For completeness it is important to note that there are many other ways of defining the fractional derivative. This is one of the issues with using the fractional derivative operator in that it is not clear which definition to take. We however will only be using the Grunwald definition as previously stated as we can easily obtain a finite difference numerical method from it.

Perhaps the most commonly used of these other definitions is the Reimann-Liouville definition

$$\frac{d^\alpha f(x)}{dx^\alpha} \equiv D_+^\alpha f(x) = \frac{1}{\Gamma(n-\alpha)} \frac{d^n}{dx^n} \int_{-\infty}^x (x-\xi)^{n-\alpha-1} f(\xi) d\xi, \quad (3.5)$$

which is defined over the domain $[-\infty, x]$. Another definition is known as the Weyl partial integral

$$\frac{d^\alpha f(x)}{d(-x)^\alpha} \equiv D_-^\alpha f(x) = \frac{(-1)^n}{\Gamma(n-\alpha)} \frac{d^n}{dx^n} \int_x^\infty (\xi-x)^{n-\alpha-1} f(\xi) d\xi, \quad (3.6)$$

which is defined over the domain $[x, \infty]$. Eqs. (3.5).(3.6) can then be shortened to the following

$$D_{\pm}^{\alpha} f(x) = \frac{(\pm 1)^n}{\Gamma(n - \alpha)} \frac{d^n}{dx^n} \int_0^{\infty} \xi^{n-\alpha-1} f(x \mp \xi) d\xi, \quad (3.7)$$

in these cases n is the smallest integer larger than the real number α see [1] for these definitions.

We can see some equivalence in these definitions as under certain conditions we can obtain the Grunwald sum from the Riemann-Louville definition. These certain conditions are that we take $n = 0$ so we have,

$$D_{\pm}^{\alpha} f(x) = \frac{1}{\Gamma(-\alpha)} \int_0^{\infty} \xi^{-\alpha-1} f(x \mp \xi) d\xi. \quad (3.8)$$

We can then represent the integral as a sum, if we take h to be the step size, then ξ can be represented as a number of these steps say kh . Eq. (3.8) now becomes,

$$\frac{1}{\Gamma(-\alpha)} \sum_{k=0}^N (kh)^{-\alpha-1} f(x \mp kh) h.$$

It is then proved in [10] that as $k \rightarrow \infty$,

$$\frac{\Gamma(k - \alpha)}{\Gamma(k + 1)} \approx k^{-\alpha-1}.$$

Using this we then get our derivative as

$$\frac{1}{h^{\alpha}} \sum_{k=0}^N \frac{\Gamma(k - \alpha)}{\Gamma(-\alpha)\Gamma(k + 1)} f(x \mp kh),$$

which is the Grunwald sum defined earlier.

There are also some other definitions for the fractional derivative which are not quite so general for example Liouville defined a derivative for functions expressed

as a series expansion if exponentials [12]. If

$$f = \sum c_j e^{b_j x}, \quad (3.9)$$

the derivative can then be expressed as,

$$\frac{d^\alpha f}{dx^\alpha} \equiv \sum_{j=0}^{\infty} c_j b_j^\alpha e^{b_j x}. \quad (3.10)$$

3.3 Standard Derivatives

If we are to develop a spectral method to numerically model the fractional diffusion equation then we need derivatives for functions such as $\cos(x)$, $\sin(x)$ and e^x . Firstly we shall look at the fractional derivative for $\cos(x)$, [12] gives the derivative as,

$$\frac{d^\alpha}{dx^\alpha} \cos(x) = \cos\left(x + \frac{\pi\alpha}{2}\right) + \frac{x^{-2-\alpha}}{\Gamma(-\alpha-1)} - \frac{x^{-4-\alpha}}{\Gamma(-\alpha-3)} + \dots \quad (3.11)$$

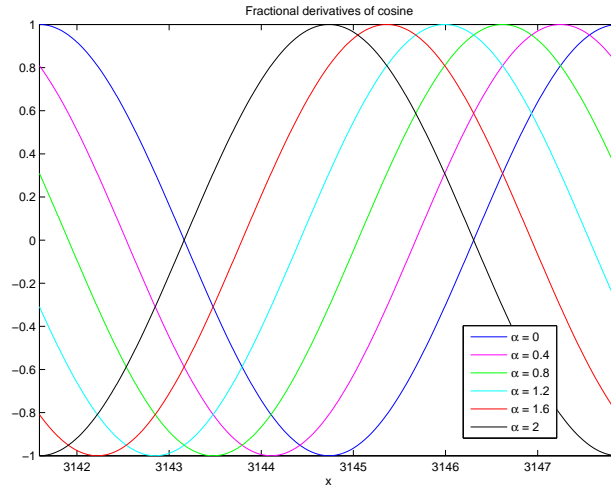
however Eq. (3.11) is only valid for large x , i.e. x that is approaching the infinity limit. Fig. 3.1 gives a range derivatives for α ranging from 0.4 up to 2. We can see that as α increases the value of the derivative gets closer to the second order derivative which is $-\cos(x)$.

The definition for the fractional derivative of $\sin(x)$ is given as,

$$\frac{d^\alpha}{dx^\alpha} \sin(x) = \sin\left(x + \frac{\pi\alpha}{2}\right) + \frac{x^{-1-\alpha}}{\Gamma(-\alpha)} - \frac{x^{-3-\alpha}}{\Gamma(-\alpha-2)} + \dots \quad (3.12)$$

again this is only valid for large x . Fig. 3.2 gives the same range of fractional derivatives for $\sin(x)$ as Fig. 3.1 does for $\cos(x)$, again we can see that as α increases the derivatives get closer to the second order derivative.

It would be beneficial to us to have a definition that is valid for any value of x . In [8] the fractional derivative for $\sin(x)$ is given as just the first term of the expansion in Eq. (3.12) applying this idea to the $\cos(x)$ derivative as well we get

Figure 3.1: Various fractional derivatives of $\cos(x)$

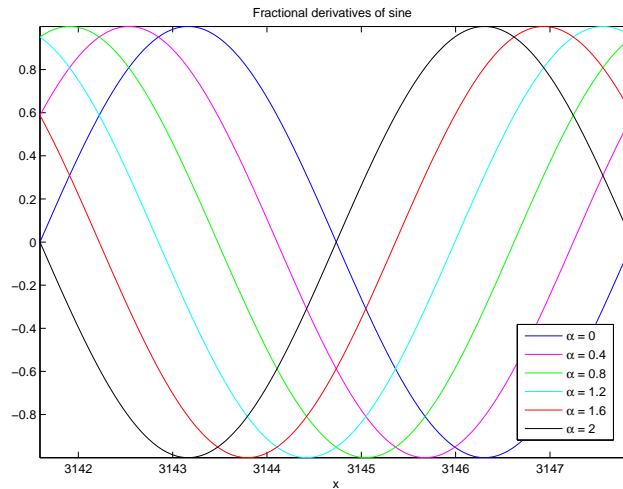
the following as our definitions for the fractional derivatives of $\cos(x)$ and $\sin(x)$,

$$\frac{d^\alpha}{dx^\alpha} \cos(x) = \cos\left(x + \frac{\pi\alpha}{2}\right), \quad (3.13)$$

$$\frac{d^\alpha}{dx^\alpha} \sin(x) = \sin\left(x + \frac{\pi\alpha}{2}\right). \quad (3.14)$$

Using Eqs. (3.13).(3.14) we can produce similar graphs to Fig. 3.1 and Fig. 3.2 when doing this we find that the results look very much the same over the domain. We can also use these definitions on domains with small x see Fig. 3.3(a) and Fig. 3.3(b).

Since we require these definitions for use in the spectral method we will assess the suitability of using the different definitions once we have obtained our numerical solution or not. We can then decide whether to just use the shortened definitions. If not then another option to allow us to use any domain is to consider a transform

Figure 3.2: Various fractional derivatives of $\sin(x)$

of the x domain to one that has larger values e.g. by adding 1000 to each x value. We have to then wonder if this will give us the same results that would have been obtained on the original domain.

We can also define a fractional derivative for the exponential function as,

$$\frac{d^\alpha}{dx^\alpha} e^{\lambda x} = \lambda^\alpha e^{\lambda x}, \quad (3.15)$$

see [8].

3.4 Binomial Coefficients and Gamma Functions

As previously discussed the binomial coefficient is equivalent to a series of Gamma functions, we call this the weight and define it as,

$$w_k = \frac{\Gamma(k - \alpha)}{\Gamma(k + 1)\Gamma(-\alpha)}. \quad (3.16)$$

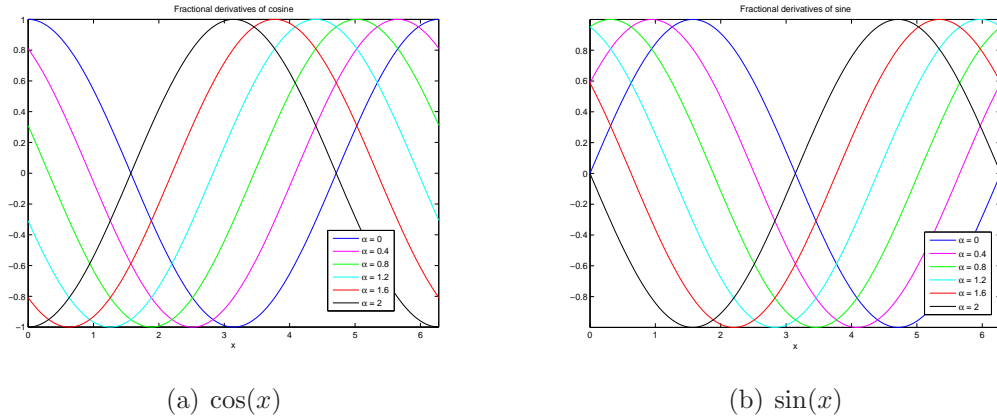


Figure 3.3: Various Fractional Derivatives with small x

These weights are worked out for each k in the sum, and their value gradually decreases as k increases Fig. 3.4 shows the weights when $\alpha = 1.5$ and $\alpha = 2$ for k up to 10. The sum to ∞ is still valid when $\alpha = 2$, this will become clear in Eq. (3.17). In this w_k will equal zero when $k = \alpha + 1$ and for all k after.

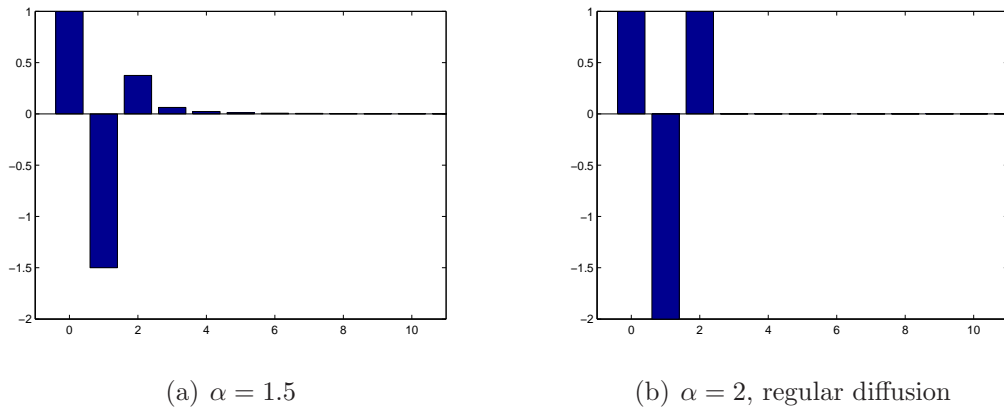


Figure 3.4: Examples of weights

Comparing these two sets of values we see the fractional case puts more weight on values for larger k indicating a much more global solution. If we now go back to our turbulent flow with rotating eddies, the velocity fluctuations would allow

transport of particles further than the immediate points. These weights indicate that using fractional diffusion could be a good model for diffusion in turbulent flows.

When it comes to developing our finite difference scheme it is beneficial to use the same definition of the weights for both fractional and regular diffusion. However, this presents a problem if we use Eq. (3.16) since the Gamma function is not defined for negative integers, see Fig. 3.5.

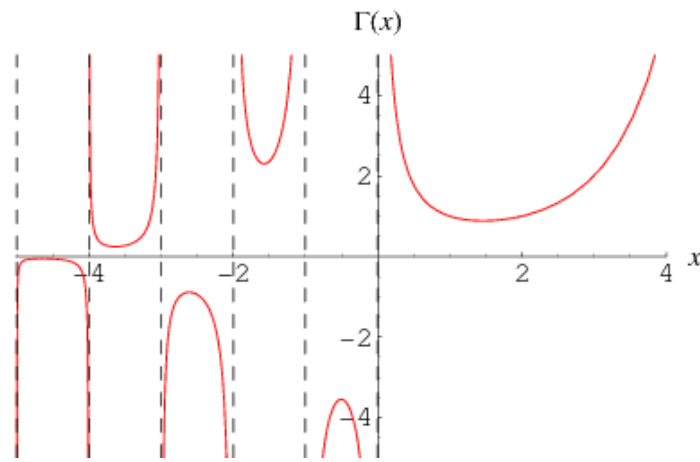


Figure 3.5: Plot of Gamma functions, [16]

To allow us to use the same definition for both cases we use Eq. (3.17) for the weights as given by Meerschaert and Tadjeran [10].

$$\begin{aligned}
 w_0 &= 1 \\
 w_1 &= -\alpha \\
 w_k &= \frac{(-\alpha)(-\alpha+1)\dots(-\alpha+k-1)}{k!} \text{ for all } k \geq 2,
 \end{aligned} \tag{3.17}$$

This can be derived from Eq. (3.16) to do this we use the gamma function recursion relationship,

$$\Gamma(x+1) = x\Gamma(x), \tag{3.18}$$

and its reflection identity,

$$\Gamma(-x) = \frac{-\pi \operatorname{cosec}(\pi x)}{\Gamma(x+1)}. \quad (3.19)$$

To show how this works we will look at a select few cases for $k = 0, 1$. Taking $k = 0$ we get the weight as,

$$w_0 = \frac{\Gamma(-\alpha)}{\Gamma(-\alpha)\Gamma(1)}$$

for an integer we have,

$$\Gamma(n) = \frac{n!}{n}$$

and so we get $w_0 = 1$.

Moving on to $k = 1$ we have the weight as,

$$w_1 = \frac{\Gamma(1-\alpha)}{\Gamma(-\alpha)\Gamma(2)},$$

using the reflection identity Eq. (3.19) we get,

$$w_1 = \frac{\Gamma(1-\alpha)\Gamma(\alpha+1)}{-\pi \operatorname{cosec}(\pi x)},$$

then using the recursion relationship Eq. (3.18) and the reflection identity again we get,

$$w_1 = \frac{-\alpha\Gamma(\alpha+1)(-\pi \operatorname{cosec}(\pi x))}{\Gamma(\alpha+1)(-\pi \operatorname{cosec}(\pi x))},$$

which cancels down to give $w_1 = -\alpha$.

To get the general formula multiple applications of the recursion relationship are required to break down the $\Gamma(k-\alpha)$ term.

Chapter 4

Finite Difference Approximations

The majority of methods to solve the fractional diffusion equation use a finite difference approach see [10, 9, 15].

4.1 Numerical Approximation

Although the definitions for fractional derivatives suggest a finite difference scheme should be straight forward to develop, it is important to take make sure the scheme becomes the usual central difference scheme for a second order derivative

$$\frac{\partial^2 c}{\partial x^2} \approx \frac{c_{i-1} - 2c_i + c_{i+1}}{\Delta x^2},$$

when $\alpha = 2$.

Using the previously given definitions this is not the case, it is proved by Meerschaert and Tadjeran [10] that this method is unstable. This paper goes on to prove that using what is known as a right shifted Grunwald approximation Eq. (4.1) produces a stable result. It only looks at using Riemann derivative so takes values on the left side of the domain into account. We will extend this to use the central definition previously given.

Our new shifted definitions for the fractional derivative are,

$$\frac{d^\alpha f}{dx^\alpha} \equiv \lim_{\Delta x \rightarrow 0} \frac{1}{\Delta x^\alpha} \left(\sum_{k=0}^{\infty} \frac{\Gamma(k-\alpha)}{\Gamma(-\alpha)\Gamma(k+1)} f(x - (k-1)\Delta x) \right) \quad (4.1)$$

and

$$\frac{d^\alpha f}{d(-x)^\alpha} \equiv \lim_{\Delta x \rightarrow 0} \frac{1}{\Delta x^\alpha} \left(\sum_{k=0}^{\infty} \frac{\Gamma(k-\alpha)}{\Gamma(-\alpha)\Gamma(k+1)} f(x + (k-1)\Delta x) \right). \quad (4.2)$$

We can now develop our numerical approximations for these definitions. Eq. (4.1) is valid on $-\infty$ to x and so refers to the left side of the domain. We can approximate this using,

$$\sum_{k=0}^i \frac{w_k f_{i-(k-1)}}{\Delta x^\alpha}, \quad (4.3)$$

where the subscript i refers to the position of x in the domain and Δx is the size of the space step. Here, because we just want to use the left side of the domain the sum goes from 0 to i . The equivalent approximation for the right side of the domain is,

$$\sum_{k=0}^{N-i} \frac{w_k f_{i+(k-1)}}{\Delta x^\alpha}. \quad (4.4)$$

This approximation uses values on the right side of the domain so the sum goes from i to N , where $N\Delta x = R$, R is the right hand boundary of the domain. Initially we will make the probability of a particle jumping forwards or backwards equal, therefore in Eq. (3.4) $\beta = 0$. If we also discretize the time derivative we get Eq. (4.5) as our approximation for the fractional diffusion equation.

$$c_i^{n+1} = c_i^n + \frac{K_\alpha \Delta t}{\Delta x^\alpha} \left(\frac{1}{2} \sum_{k=0}^i w_k c_{i-(k-1)}^n + \frac{1}{2} \sum_{k=0}^{N-i} w_k c_{i+(k-1)}^n \right), \quad (4.5)$$

where n refers to the time step. This gives us an explicit scheme for the fractional diffusion equation. Which can be solved for each space step to give the value of

the concentrate for the next time step. We then be repeate for however many time steps we require, with the chosen boundary conditions being applied at each stage. Meerschaert, Tadjeran and Scheffler [10, 15] look at implicit and semi implicit methods and the stability regions for the methods. Developed in [15] is an equivalent Crank-Nicolson method for the fractional diffusion term. We however will only consider the explicit case for ease of implementation and to allow us to move on to other methods.

This method is easily extended to two dimensions. Schemes for doing this are explored by Meerschaert, Tadjeran and Scheffler [9]. The basic way to extend the scheme we already have is to just use another summation for the y derivative. Using this fractional approach does not limit us to using the same value for α for both x and y derivatives, we can use different values that allow us to have a more variable model for diffusion. Therefore we now want to approximate the equation,

$$\frac{\partial c}{\partial t} = K_\alpha \frac{\partial^\alpha c}{\partial x^\alpha} + D_\eta \frac{\partial^\eta c}{\partial x^\eta} \quad (4.6)$$

where $1 \leq \alpha \leq 2$ and $1 \leq \eta \leq 2$ and K_α, D_η are the diffusivity constants for either the x or y dimension. This is easily done by using the ideas developed in the previous section giving us our numerical scheme as,

$$\begin{aligned} c_{i,j}^{n+1} = c_{i,j}^n &+ \frac{K_\alpha \Delta t}{\Delta x^\alpha} \left(\frac{1}{2} \sum_{k=0}^i w_k c_{i-(k-1),j}^n + \frac{1}{2} \sum_{k=0}^{N-i} w_k c_{i+(k-1),j}^n \right) \\ &+ \frac{D_\eta \Delta t}{\Delta x^\eta} \left(\frac{1}{2} \sum_{k=0}^j w_k c_{i,j-(k-1)}^n + \frac{1}{2} \sum_{k=0}^{N-j} w_k c_{i,j+(k-1)}^n \right). \end{aligned} \quad (4.7)$$

Here i denotes the x position, j denotes the y position and n denotes the time step. Again we have a set of equations to be solved to get the value of c at each space point for a specific time step.

Eq. (4.8) uses four summations and gives equal diffusion in left and right directions for both x and y dimensions. To alter the way in which diffusion occurs,

we can choose the required set of summations to model that particular diffusion. Further to this, we could also use a modification of our symmetric scheme in one dimension where we can pick the value of β to model the probability of a forwards or backwards jump.

4.2 A 1D Test Case

Our scheme Eq. (4.5) involves two summations, each refer to a different part of the domain. For the purpose of testing our scheme we will split it into two schemes one used for the left side of the domain and the other used on the right side.

4.2.1 Left Scheme Test

In order to check that our scheme is working correctly we can compare it to an example with an analytic result given in [15]. The example provided only uses the left derivative defined over $[-\infty, x]$ and is given as,

$$\frac{\partial u(x, t)}{\partial t} = d(x) \frac{\partial^{1.8} u(x, t)}{\partial x^{1.8}} + q(x, t)$$

on the domain $0 < x < 1$, with diffusion coefficient

$$d(x) = \Gamma(2.2)x^{2.8}/6,$$

the source function

$$q(x, t) = -(1 + x)e^{-t}x^3,$$

initial condition

$$u(x, 0) = x^3 \quad \text{for } 0 < x < 1$$

and boundary conditions

$$u(0, t) = 0, u(1, t) = e^{-t} \quad \text{for } t > 0.$$

This has the exact solution

$$u(x, t) = e^{-t}x^3.$$

4.2.2 Right Scheme Test

To check the right sided derivative we can modify this example by replacing the x with $1 - x$. This gives us a suitable function that the right sided derivative will work for. The example we use now becomes,

$$\frac{\partial u(x, t)}{\partial t} = d(x) \frac{\partial^{1.8} u(x, t)}{\partial x^{1.8}} + q(x, t)$$

on the domain $0 < x < 1$, with diffusion coefficient

$$d(x) = \Gamma(2.2)(1 - x)^{2.8}/6,$$

the source function

$$q(x, t) = -(1 + (1 - x))e^{-t}(1 - x)^3,$$

initial condition

$$u(x, 0) = (1 - x)^3 \quad \text{for } 0 < x < 1$$

and boundary conditions

$$u(0, t) = e^{-t}, u(1, t) = 0 \quad \text{for } t > 0.$$

This has the exact solution

$$u(x, t) = e^{-t}(1 - x)^3.$$

The graphs in Fig. 4.1 give plots of the numerical solution with the analytical solution for a final time of 1 second, so the analytical solutions become $u(x, 1) = x^3/e$ and $u(x, 1) = (1 - x)^3/e$ respectively. These use a space step of 0.1 and a time step

of 0.0001. We see that numerical scheme is producing a result close to that of the analytical solution. The accuracy of this can be improved by changing the values of the time and space steps and will be assessed later. However from using these values, we can still see that the numerical scheme is producing what we would expect and is therefore working correctly. This gives us confidence both to proceed with the central difference case and in the validity of any results we obtain from it.

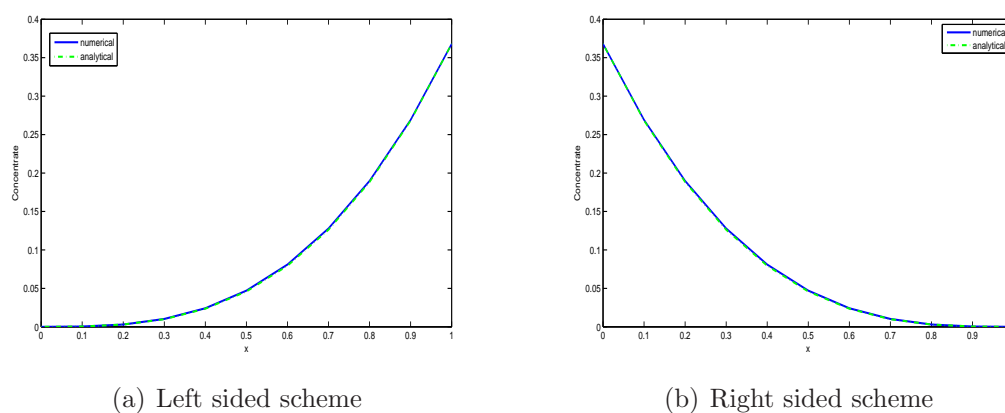


Figure 4.1: Numerical and analytical results

4.2.3 Accuracy of the Schemes

Since we have a numerical and analytical solution for both the left and right schemes, we can now assess their accuracy. We do this by looking at the error between the numerical solution and the analytical solution when fixing the time step and changing the space step. The error is calculated by taking the sum of the difference between the numerical solution and the analytical solution at each point squared and then normalizing this by dividing by the sum of the analytical solution

at each point squared. This is perhaps best given in the following expression,

$$\text{error} = \left(\frac{\int (e_a - e_n)^2 dx}{\int e_a^2 dx} \right)^{\frac{1}{2}}. \quad (4.8)$$

This is known as the L_2 error.

We then fix the time step at 0.0001, change the space step and calculate the error Eq. (4.8) for each space step. The results for space steps between 1/10 and 1/100 are given in Tab. 4.1.

Δx	left error	right error
1/10	0.0059	0.0059
1/20	0.0032	0.0032
1/30	0.0022	0.0022
1/40	0.0017	0.0017
1/50	0.0014	0.0014
1/60	0.0011	0.0011
1/70	0.001	0.001
1/80	0.0009	0.0009
1/90	0.0008	0.0008
1/100	0.0007	0.0007

Table 4.1: Error for left and right sided schemes

We only have an analytical solution for one sided problems and so the errors are calculated using either the left or right sided derivative, however we can see that both schemes give the same error. If we then plot these results on a log log scale we can get the convergence rate that is almost linear, see Fig. 4.2.

4.2.4 Stability

We now consider the stability of the schemes, notice that for the error analysis we used a time step of 0.0001. This allows us to obtain a stable solution for all sizes

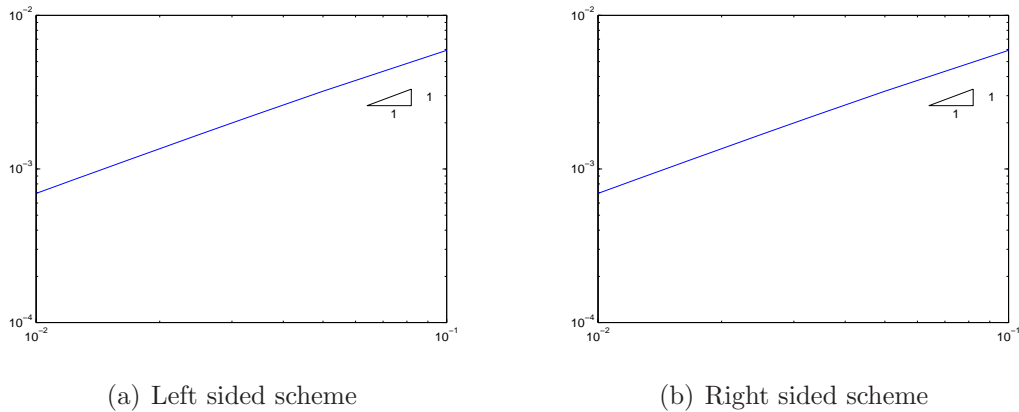


Figure 4.2: Convergence rates

of the space step. Any larger time step would have meant an unstable solution when the Δx got smaller. This means that these schemes are conditionally stable with what looks like a small stability region. We can also look at the stability for our central scheme. Unconditionally stable methods have been constructed by using an equivalent Crank-Nicolson scheme for the fractional diffusion equation, see [15]. This paper concentrates on using the method for the left derivative only. It does mention that it is possible to extend the method for use with the central derivative but it increases the computation time.

4.3 A 2D Test Case

As for one dimension we can also find a test example for the two dimensional case. A test case is provided in [9], for this we will need to use the left sided summations for both the x and y directions. Like the one dimensional case this can be modified by changing either x or y for $(1 - x)$ or $(1 - y)$ in the example and selecting the right or left summations required in the numerical scheme. This would provide us with four schemes to test, since we have tested the right and left schemes in the one dimensional case and we are using the same summations developed for this we only present the solutions to the one test case.

4.3.1 Test of 2D Scheme

The example we use to test our numerical scheme as given in [9] is as follows, the fractional differential equation we wish to solve is,

$$\frac{\partial u(x, y, t)}{\partial t} = d(x, y) \frac{\partial^{1.8} u(x, y, t)}{\partial x^{1.8}} + e(x, y) \frac{\partial^{1.6} u(x, y, t)}{\partial y^{1.6}} + q(x, y, t).$$

This is defined on a rectangular domain $0 < x < 1$, $0 < y < 1$ for time $0 \leq t \leq 1$. The diffusion coefficients $d(x, y)$ and $e(x, y)$ are given as,

$$d(x, y) = \Gamma(2.2)x^{2.8}y/6 = 0.18363375x^{2.8}y,$$

$$e(x, y) = 2xy^{2.6}/\Gamma(4.6) = 0.1494624672xy^{2.6}.$$

The forcing function $q(x, y, t)$ is,

$$q(x, y, t) = -(1 + 2xy)e^{-t}x^3y^{3.6},$$

all subject to the Dirichlet boundary conditions $u(0, y, t) = u(x, 0, t) = 0$, $u(1, y, t) = e^{-t}y^{3.6}$ and $u(x, 1, t) = e^{-t}x^3$. The exact solution to this problem is given by,

$$u(x, y, t) = e^{-t}x^3y^{3.6}.$$

We will only be looking at the result up to a final time of $t = 1$ so the solution we want our numerical scheme to produce is,

$$u(x, y, t) = \frac{x^3y^{3.6}}{e}.$$

To obtain our numerical result the scheme we will be using is,

$$u_{i,j}^{n+1} = u_{i,j}^n + \frac{d_{i,j}\Delta t}{\Delta x^{1.8}} \left(\sum_{k=0}^i w_k C_{i-(k-1),j}^n \right) + \frac{e_{i,j}\Delta t}{\Delta y^{1.6}} \left(\sum_{k=0}^j w_k C_{i,j-(k-1)}^n \right) + q_{i,j}^n.$$

We set the time step $\Delta t = 0.001$ and the space steps $\Delta x = \Delta y = 0.1$ and run up to a final time of one second. Fig. 4.3 and Fig. 4.4 show the numerical and analytical solutions to the example.

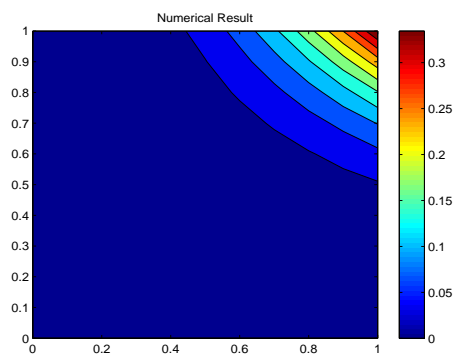


Figure 4.3: Numerical Result

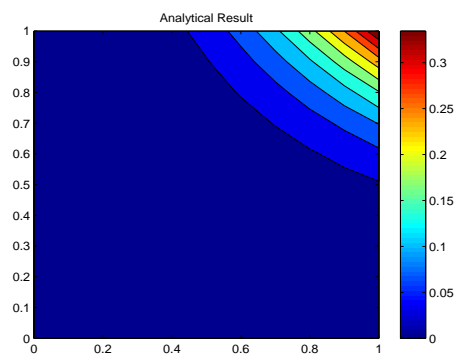


Figure 4.4: Analytical result

From the figures the solutions look very similar and it is not clear what the difference between them is. To illustrate this, Fig. 4.5 is a plot of the analytical solution minus the numerical solution, there are some differences in the solution which is to be expected due to the accuracy of the numerical scheme. However, the differences are very small indicating that the scheme is a good approximation to the analytical result.

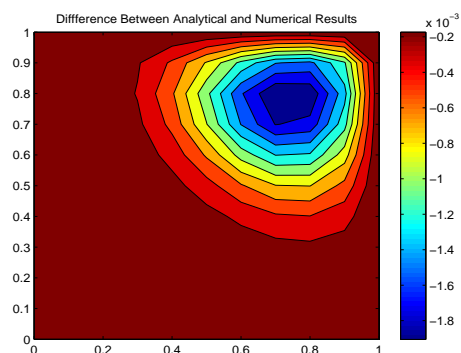


Figure 4.5: Difference between analytical and numerical results

4.3.2 Accuracy

To assess the accuracy of the scheme, we use the same method as for one dimension but instead of using the single integral in Eq. (4.8) we use a double integral so that our global error can now be calculated by,

$$error = \left(\frac{\int \int (e_a - e_n)^2 dx dy}{\int \int (e_a)^2 dx dy} \right)^{\frac{1}{2}}. \quad (4.9)$$

Fixing the time step to $\Delta t = 0.001$ and running the program for each different space steps keeping $\Delta x = \Delta y$ we find the errors given to Tab. 4.2. The space step

$\Delta x = \Delta y$	error
1/10	0.0027
1/20	0.0012
1/30	0.0007
1/40	0.0005
1/50	0.0004
1/60	0.0003

Table 4.2: Error for two dimensional scheme

has not been made as small as for one dimension this is because a smaller time step is then required to get a stable solution which greatly increases the computation time. The values can still be plotted on a log log scale as in Fig. 4.6 to give us an idea of the convergence rate which is very close to linear.

4.4 The 1D Central Scheme Results

If we now consider symmetric initial data, we will take a Gaussian distribution with mean of 20π and standard deviation of four defined on the domain $0 < x < 40\pi$, see Fig. 4.7. We are using a large domain so the diffusion does not interact with the boundary.

To begin with we will use the left or right definition separately, this is the equiva-

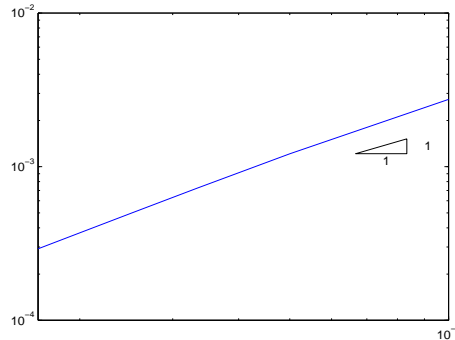


Figure 4.6: Convergence rate for the 2D test case

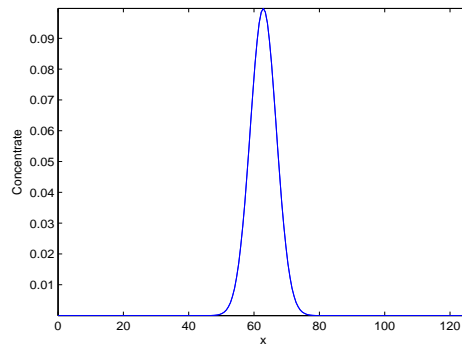


Figure 4.7: Initial data in the form of a normal distribtuion

lent of setting $\beta = -1$ or 1 in Eq. (3.4). Physically what we are encouraging here is either a strong leftwards diffusion or a strong rightwards diffusion, the strength of which can be altered by changing the value of α . We see that a lower value of α produces a greater amount of diffusion, as well as a stronger skew on the concentrate in either direction depending on the scheme. The left and right schemes produce the mirror image of each other for the same values of α see Fig. 4.8 . The boundary conditions have been set to $\frac{\partial}{\partial x}c(0, t) = 0$ and $\frac{\partial}{\partial x}c(40\pi, t) = 0$. The diffusion coefficient has been set to one for both cases. We will run the process for a final time of 20 seconds with output every two seconds.

To get a scheme that diffuses symmetrically, we set $\beta = 0$ in Eq. (3.4). Physically

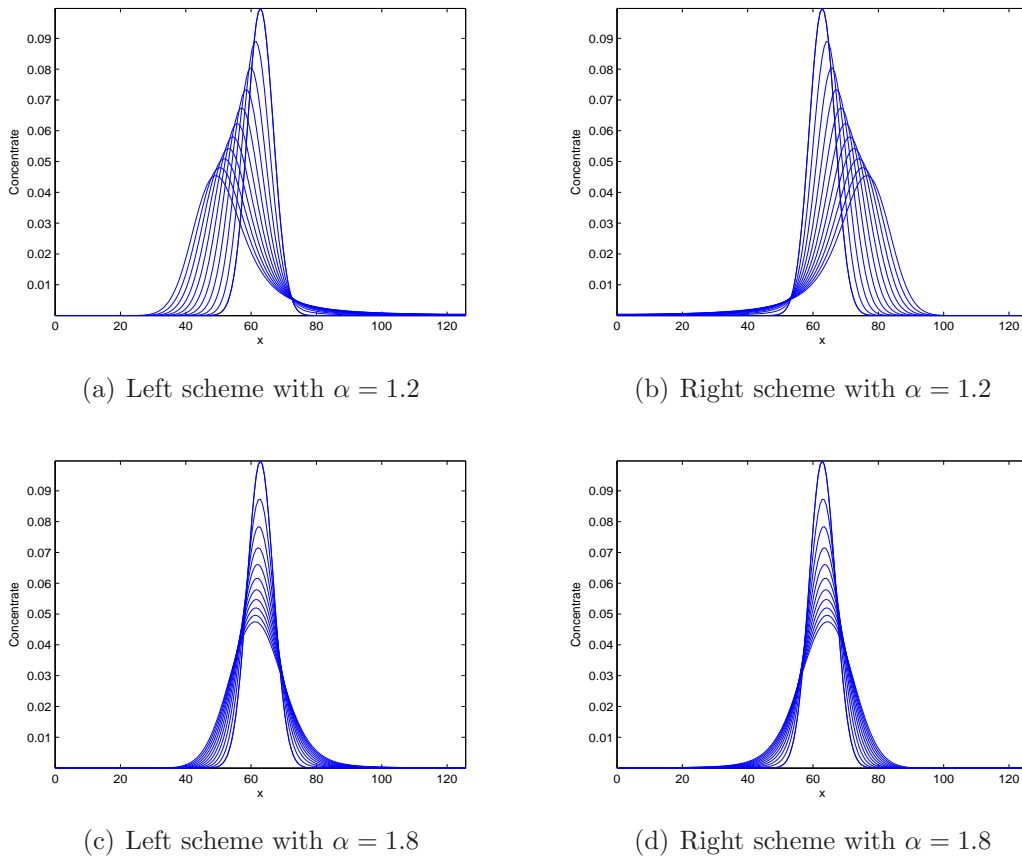


Figure 4.8: Fractional diffusion using only left or right schemes

we are saying here that the probability of a particle diffusing in any direction is equal. We now look at the diffusion for various values of α and compare it to ordinary diffusion. See Fig. 4.4 for fractional diffusion with various values of α .

From these it is unclear what the rate diffusion at which is occurring for each values of α . To assess this we calculate the standard deviation of the diffusing plume as time progresses Fig. 4.10 illustrates this. It does not quite show what we were expecting, but for all selected values of α the fractional diffusion occurs at a faster rate than ordinary diffusion. This also gives us some values to compare to our spectral method to check that it is giving us the same results as the finite difference method.

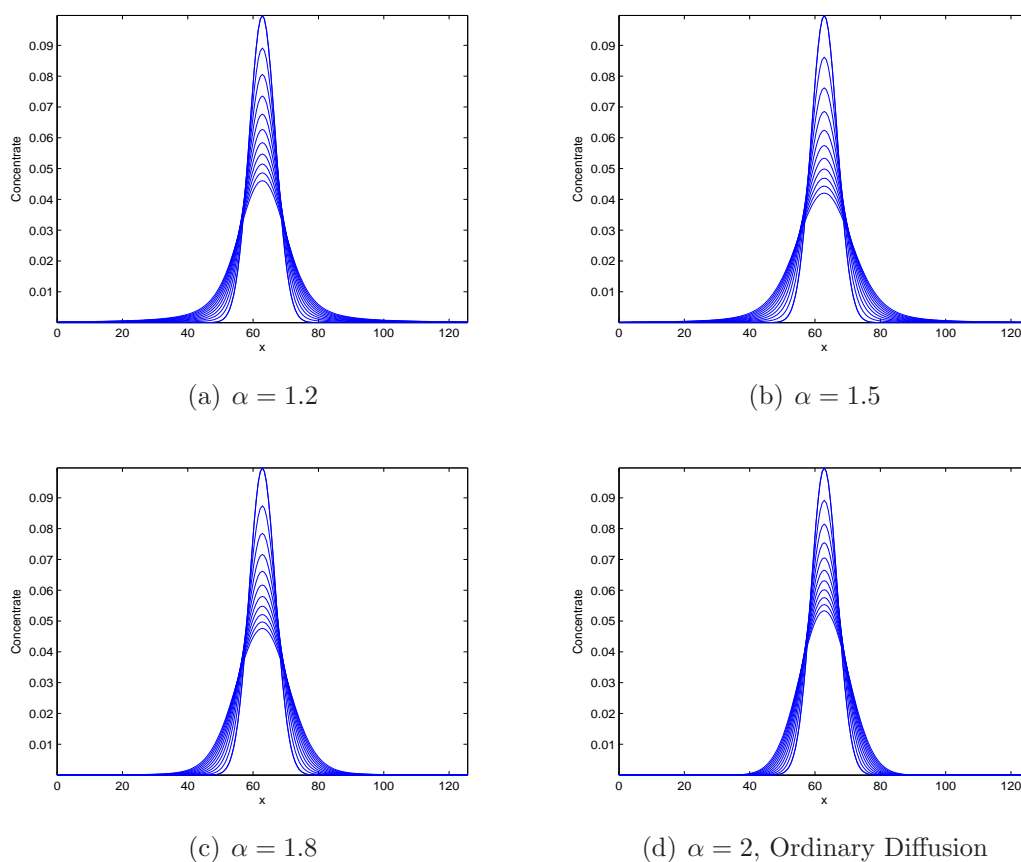


Figure 4.9: Results using the central scheme for various values of α

In fact as the domain gets the larger diffusion rates get closer to those we were expecting. We also see that the closer α gets to one then a larger domain is required to get the faster diffusion rates. This makes comparison between different values of α difficult as we need to make sure the domain is large enough to allow faster diffusion for small values of α and slower for large values of α . In Fig. 4.10 we see that we have made the domain large enough so that the values of α we are comparing have faster diffusion rates for the lower α . We will also notice when it comes to the spectral method that the solutions only coincide with the finite difference scheme up until the diffusion reaches the boundary. This would imply that as

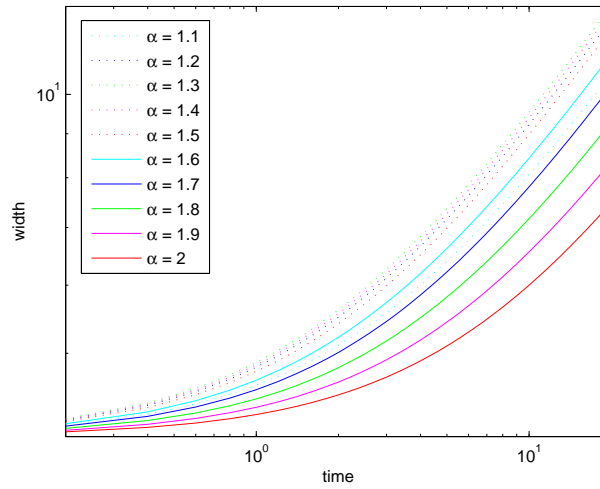


Figure 4.10: Width of diffusing plume plotted on loglog scale

long as we are diffusing a concentrate in a medium that doesn't have boundaries, i.e the atmosphere, then using this fractional diffusion scheme is valid. However greater investigation needs to go into looking at the effects of using a very large domain.

4.5 Two Dimensional Results

To generate results for the two dimensional case the initial data will consist of an amount of concentrate on the left side of the domain, see Fig. 4.11 for details. To begin with we will calculate our numerical results for the second order diffusion equation case, using the scheme Eq. (4.8) this gives us a base value to compare other results too. To do this we use the domain $0 \leq x \leq 10$, $0 \leq y \leq 10$, space steps of $\Delta x = \Delta y = 0.1$, a time step of $\Delta t = 0.001$ and a final time of $t = 2$ seconds, see Fig. 4.12.

The scheme we have developed for the two dimensional case can be altered in a number of ways to change the rate of the diffusion. The most obvious of these being that we can alter the fractional value of the diffusion. However, we can also

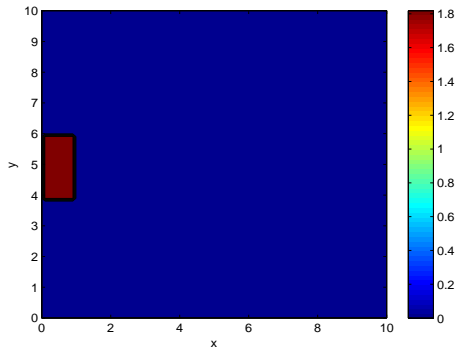


Figure 4.11: Initial Data

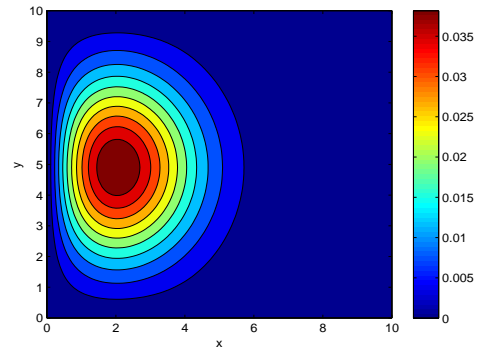
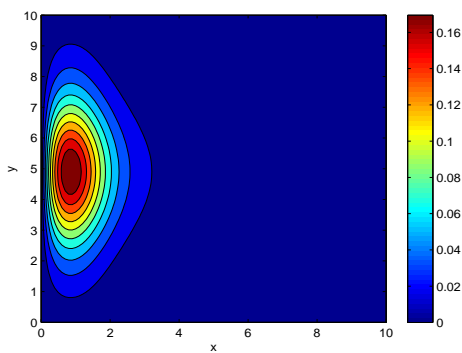
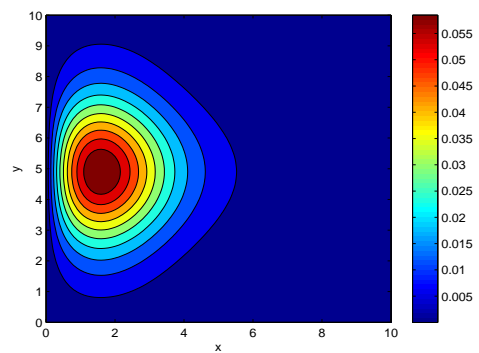


Figure 4.12: Second order diffusion

change the scheme so that we don't use all four summations. Since our initial data is symmetric in the y direction, we will use both left and right summations in this direction. To compare results more easily we fix the fractional value on the y derivative to 1.5. It is then the x derivative we will make the changes to. Fig. 4.13 shows the results using a central scheme in the x direction, Fig. 4.14 uses the left scheme and Fig. 4.15 uses the right scheme. For all three, the results are calculated using a fractional value of 1.2 and 1.6 in the x derivative.

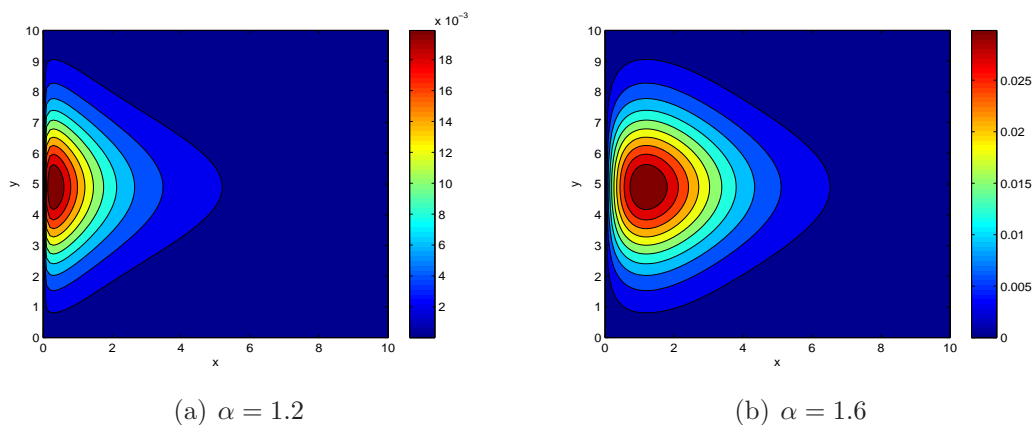
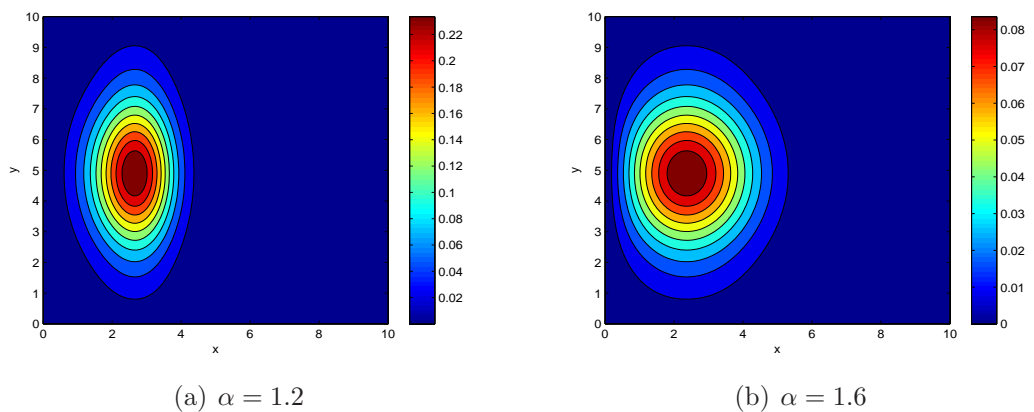


(a) $\alpha = 1.2$



(b) $\alpha = 1.6$

Figure 4.13: Two dimensions using a central scheme in x

Figure 4.14: Two dimensions using a left scheme in x Figure 4.15: Two dimensional using a right scheme in x

We get a very different pattern to the diffusion depending on the scheme and the value for α we use. Therefore it is possible to pick the values to fit a physical situation. However, for the central and right scheme there is less diffusion for lower α we were expecting for. Therefore it is questionable whether these schemes should be used for this initial data, perhaps if most of the initial concentrate in on the left side of the domain we should just use the left scheme.

4.6 A 2D Advection Diffusion Plume

If we want to predict fluid motion for a concentrate introduced at the left side of a tank which advects rightwards and diffuses in the y direction we can solve the equation,

$$\frac{\partial c}{\partial t} + u \frac{\partial c}{\partial x} = K_{\eta} \frac{\partial^2 c}{\partial y^2}. \quad (4.10)$$

Again using a second order diffusion term does not give the correct rate of diffusion. An example of real situation where a dye is continuously introduced to a tank of fluid can be seen in Fig. 4.16. Here the diffusion in the y axis is due to turbulence. 'Using the second order diffusion term produces as result that looks like a parabola in the example we have more of a cone shape [5]'.
'

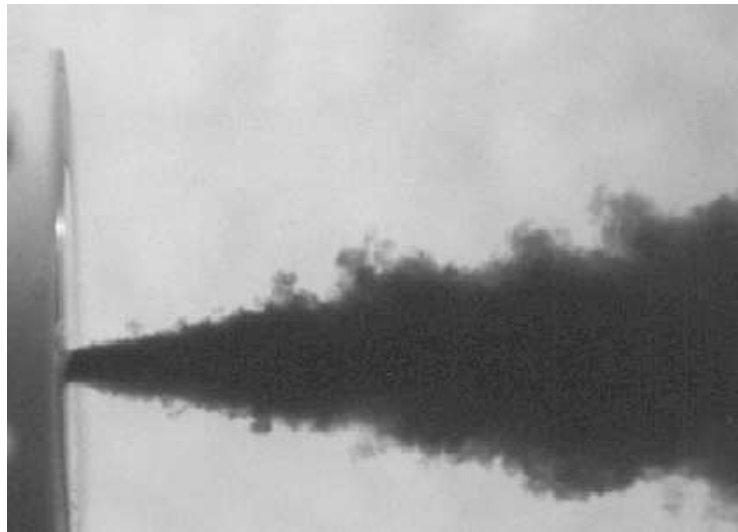


Figure 4.16: Example of an advecting plume, [5]

To create a numerical scheme we use an upwind scheme to approximate the advection term and a central fractional scheme to approximate the diffusion term. The gives us the following scheme Eq. (4.12) that produces the solution at a particular

space step for the next time step.

$$\begin{aligned}
 c_{i,j}^{n+1} &= c_{i,j}^n + \Delta t \left(-\frac{u}{\Delta x} (c_{i,j}^n - c_{i,j}^{n+1}) \right. \\
 &\quad \left. + \frac{K_\eta}{\Delta y^\eta} \left(\frac{1}{2} \sum_{k=0}^j w_k c_{i,j-(k-1)}^n + \frac{1}{2} \sum_{k=0}^{N-j} w_k c_{i,j+(k-1)}^n \right) \right)
 \end{aligned} \tag{4.11}$$

To get our numerical result we use the domain $0 \leq x \leq 10$, $0 \leq y \leq 10$ with the initial condition of a small section in the middle of the $x = 0$ axis equal to one and everywhere else equal to zero. To simulate a dye being continuously introduced into the tank we set our boundary condition so that it is one for a small section in the middle of the $x = 0$ axis and zero elsewhere. What we are doing is setting the boundary back to its initial value each time step. We do not want to allow to pass through the horizontal walls of the tank so the boundary conditions for both y axis are set to zero. To simulate fluid begin able to flow through the far boundary we use a Neumann boundary condition so $\frac{\partial}{\partial x} c(10, t) = 0$. In the solutions obtained $\Delta x = \Delta y = 0.2$, $\Delta t = 0.002$, the final time is 10 seconds, $u = 2$ and $K_\eta = 1$. See Fig. 4.17.

These are only preliminary results, further investigation needs to go into checking there validity. A start would be to calculate the width of the plume for the various values of η . Although from these we can see that as η decreases we get a result that looks more linear.

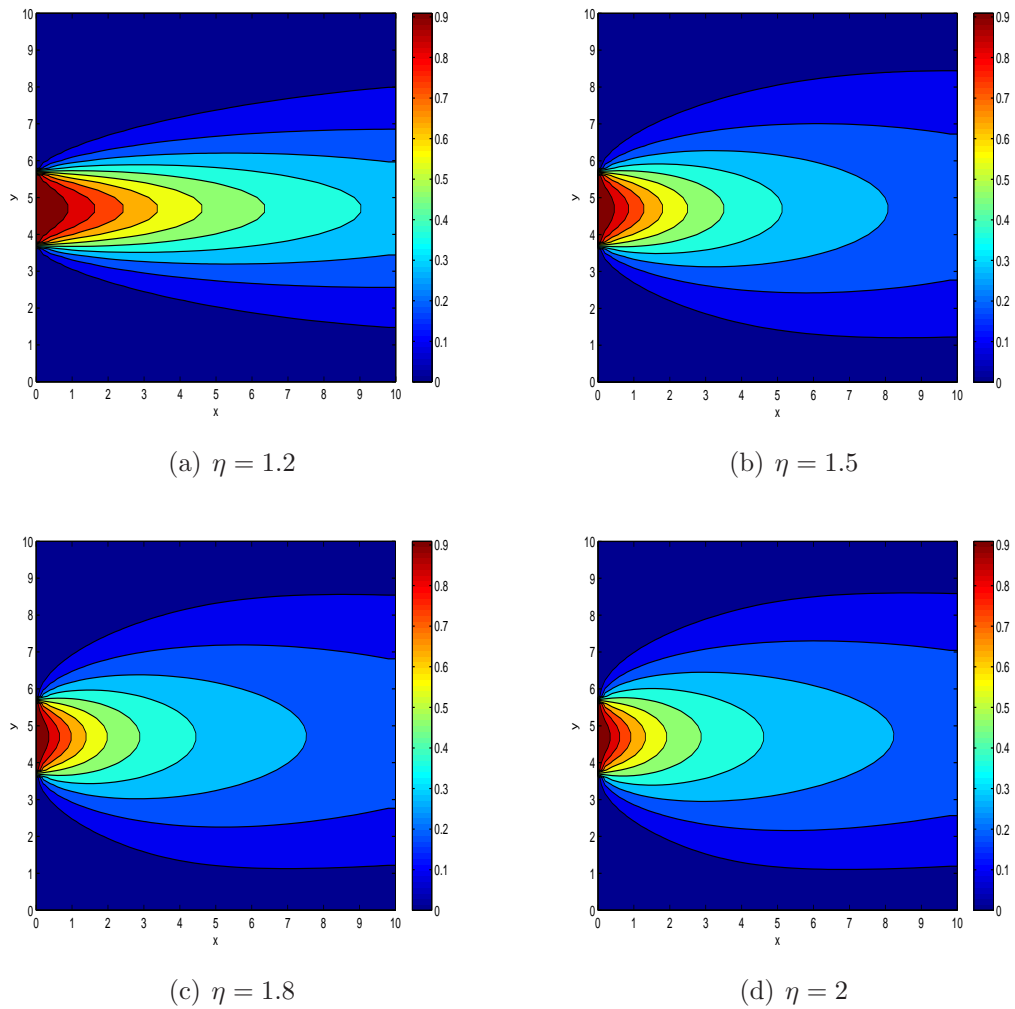


Figure 4.17: Numerical results for an advection diffusion plume

Chapter 5

A numerical scheme using Spectral Methods

We now wish to develop a spectral method to numerically calculate our solution. Our idea is that because spectral methods use global data rather than data from immediate surrounding points, they should be better suited to fractional diffusion. Fractional derivatives use data from over the entire domain so it is thought that the spectral method will produce a more accurate numerical solution. The finite difference method requires a sum over the entire domain for each discretized space step, this makes it computationally expensive. Using a spectral method should reduce the computation time as we will be using standard derivatives of the expansion functions so mean we do not have these large sums.

To begin with we will define the spectral method using the Galerkin approximation method for use with the ordinary diffusion equation. From this we can then make the modifications to the method for fractional diffusion. The book Numerical Methods for Wave Equations in Geophysical Fluid Dynamics [6] provides an understandable explanation to spectral methods, where as the book Spectral Methods Fundamentals in Single Domains [3] provides a very in depth discussion on the subject.

5.1 A spectral method for fractional diffusion

For our spectral method we want to approximate the solution to Eq. (2.4) as a series expansion,

$$c(x, t) \approx c^h(x, t) = \sum_{k=0}^N a_k(t) \varphi_k(x) \quad (5.1)$$

where the $a_k(t)$ are unknown coefficients and $\varphi_k(x)$ are expansion functions, for the value of $\varphi(x)$ we will use exponential or trigonometric functions. The spectral method works by reducing the partial differential equation (PDE) to a system of ordinary differential equations (ODEs) that have solutions $a_k(t)$. Once these are solved the approximate solution to the PDE can be obtained by substituting the $a_k(t)$ back into Eq. (5.1).

To find this system of ODEs we will take the Galerkin approximation. This requires us to use the weak formulation of Eq. (2.2) and set the residual of this to equal zero giving us the following,

$$\int_0^{2\pi} \frac{\partial c^h}{\partial t} \varphi_l(x) dx = \int_0^{2\pi} K \frac{\partial^\alpha c^h}{\partial x^\alpha} \varphi_l(x) dx \quad \text{for } l = 0, \dots, N$$

substituting in the series expansion then gives us,

$$\int_0^{2\pi} \frac{\partial}{\partial t} \left(\sum_{k=0}^N a_k(t) \varphi_k(x) \right) \varphi_l(x) dx = \int_0^{2\pi} K \frac{\partial^\alpha}{\partial x^\alpha} \left(\sum_{k=0}^N a_k(t) \varphi_k(x) \right) \varphi_l(x) dx$$

and then differentiating gives

$$\sum_{k=0}^N \frac{da_k(t)}{dt} \int_0^{2\pi} \varphi_k(x) \varphi_l(x) dx = K \sum_{k=0}^N a_k(t) \int_0^{2\pi} \frac{d^\alpha \varphi_k(x)}{dx^\alpha} \varphi_l(x) dx. \quad (5.2)$$

The functions $\varphi_k(x)$ are chosen so they are orthogonal, this mean that in Eq. (5.2) the part involving the time derivative only has a non zero values when $k = l$. Using this fact and discretizing the time derivative using an implicit Euler integration

scheme gives us the following system of ODEs,

$$\int_0^{2\pi} \varphi_l(x) \varphi_l(x) dx \left(\frac{a_l^n - a_l^{n+1}}{\Delta t} \right) = K \sum_{k=0}^N \int_0^{2\pi} \frac{d^\alpha \varphi_k(x)}{dx^\alpha} \varphi_l(x) dx a_l^{n+1}.$$

Like the finite element method we can define a mass matrix M as,

$$M_{kl} = \left(\int_0^{2\pi} \varphi_l(x) \varphi_l(x) dx \right) \delta_{kl}$$

and a stiffness or diffusivity matrix D as,

$$D_{kl} = \int_0^{2\pi} \frac{d^\alpha \varphi_k(x)}{dx^\alpha} \varphi_l(x) dx.$$

This leaves us with a matrix system in the form of,

$$(M - D\Delta t)a_l^{n+1} = Ma_l^n \tag{5.3}$$

that needs to be solved over time. Then for time steps where the actual solution is required we substitute the $a_k(t)$ into Eq. (3.9). Here we have discretized the time step implicitly but it can just as easily be solved explicitly or using any other integration scheme.

One other thing to consider is obtaining the initial condition for the $a_k(t)$ this can be formulated as so,

$$\int_0^{2\pi} \sum_{k=0}^N a_k(0) \varphi_k(x) \varphi_l(x) dx = \int_0^{2\pi} C_{init}(x) \varphi_l(x) dx$$

and again using the orthogonality condition there is only a non zero solution when $k = l$ therefore we get N initial $a_l(0)$ s given by,

$$a_l(0) = \frac{\int_0^{2\pi} C_{init}(x)\varphi_l(x)dx}{\int_0^{2\pi} \varphi_l(x)\varphi_l(x)dx}. \quad (5.4)$$

To begin with we take the domain $[0, 2\pi]$, all the derivations are shown for this domain size. However this is easily altered by changing the value of k to $k = \frac{2\pi}{\lambda}$ where $\lambda = \frac{i}{L}$. L being the length of the domain and i being the value in the summation. k still needs to be an integer so λ needs to be chosen so that it causes the π cancels out.

5.2 Choices of expansion function

Examples of expansion functions $\varphi(x)$ are $\cos(kx)$, $\sin(kx)$ combinations of the two or even e^{ikx} , for more details on possible expansion functions see [3]. Both cosine or sine only gives a valid result if we use a symmetric or antisymmetric initial condition respectively. Therefore a combination of the two would be beneficial, but this presents a problem when determining the initial conditions. Using a complex exponential would also give us as more universal method without the issue with the initial conditions. Using the definitions given in Chapter 3 we can develop numerical schemes using various expansion functions. We shall look at the results obtained from using each one, as well as the deciding whether it is acceptable to only take the shorted definitions.

5.2.1 Cosine Expansion Function

For the cosine expansion function we take $\varphi_k(x) = \cos(kx)$ and $\varphi_l(x) = \cos(lx)$ this gives the mass matrix as,

$$M_{kl} = \int_0^{2\pi} \cos(kx)\cos(lx)dx.$$

For cosine we have the orthogonality condition,

$$\int_0^{2\pi} \cos(mx)\cos(nx)dx = \begin{cases} 2\pi & \text{if } m = n \\ 0 & \text{if } m \neq n, \end{cases}$$

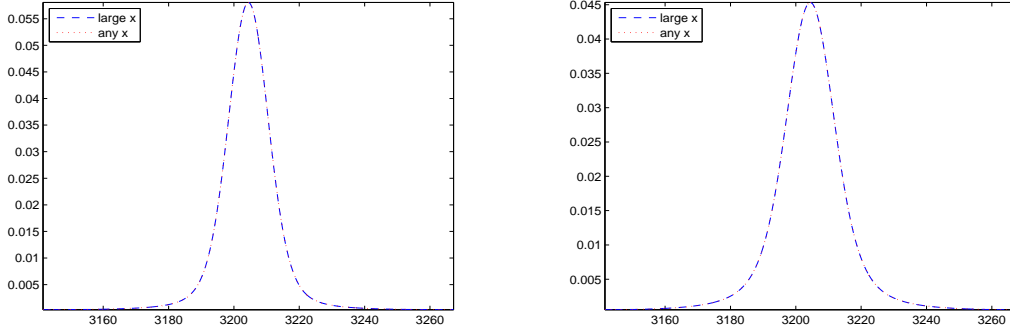
this means that the mass matrix only has diagonal entries. The stiffness matrix can be defined as,

$$D_{kl} = \int_0^{2\pi} \frac{d^\alpha \cos(kx)}{dx^\alpha} \cos(lx)dx.$$

Using the definitions for the fractional derivative of cosine we see that the orthogonality condition is no longer valid so the derivative involves a shifted cosine wave. Therefore there will be values in entries in the matrix other than in the diagonal elements, this will increase the computational time.

In Chapter 3 we gave two definitions for the fractional derivative of cosine Eq. (3.11) and Eq. (3.13). We see from an example that they both produce similar results over the same domain, in this case $1000\pi < x < 1040\pi$ which changes the integral limits on the mass and stiffness matrices to 1000 and 1040π . The initial data is a Gaussian distribution. Fig. 5.1(a) shows the results using both definitions after 10 seconds and Fig. 5.1(b) shows the results after 20 seconds. The results for both definitions are the same for both final times indicating that it is suitable to use the shortened definition Eq. (3.13) which produces results over any domain not just that of large x . Another comparison can be seen in Fig. 5.2 here we are using the domain given above when using Eq. (3.11) and the domain $0 < x < 40\pi$ is used for Eq. (3.13) the final time is 20 seconds. We see that valid results are produced which are similar, this also shows that if a transform for the derivative

had been used it result obtained would have been reasonable.



(a) Final time of 10 seconds

(b) Final time of 20 seconds

Figure 5.1: Comparison of definitions for the fractional derivative of cosine

If we use an odd function for the initial data the scheme does not produce a valid solution. We therefore need to use different expansion functions to obtain a solution.

5.2.2 Sine Expansion Function

For our expansion functions we now use $\varphi_k(x) = \sin(kx)$ and $\varphi_l(x) = \sin(lx)$ giving the mass and stiffness matrices as,

$$M_{kl} = \int_0^{2\pi} \sin(kx)\sin(lx)dx.$$

and

$$D_{kl} = \int_0^{2\pi} \frac{d^\alpha \sin(kx)}{dx^\alpha} \sin(lx)dx.$$

Sine has a similar orthogonality condition to cosine so the mass matrix again only has diagonal elements and due to the definition for the fractional derivative

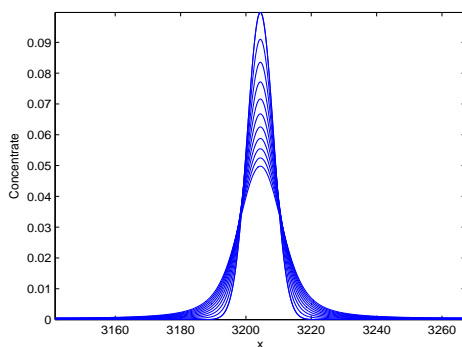
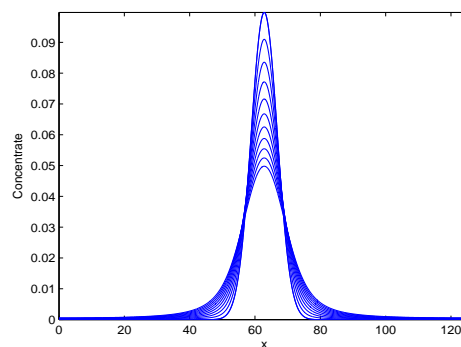
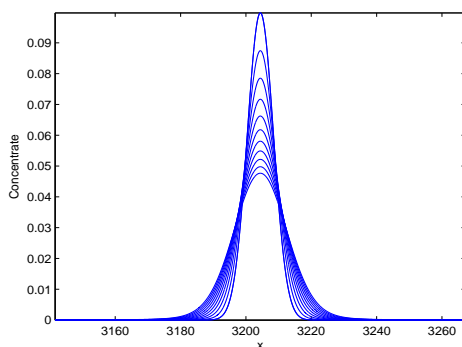
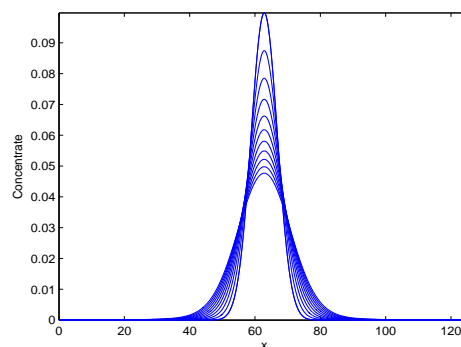
(a) $\alpha = 1.2$, definition Eq. (3.11)(b) $\alpha = 1.2$, definition Eq. (3.13)(c) $\alpha = 1.8$, definition Eq. (3.11)(d) $\alpha = 1.8$, definition Eq. (3.13)

Figure 5.2: Results for cosine expansion function using both definitions

of sine the stiffness matrix has non zero elements over the whole matrix.

Using sine as an expansion function means that the scheme is only valid for initial data that is an odd function we also find in our program for using sine that it does not transform the initial data correctly and therefore needs further work. We will not use a sine expansion function.

5.2.3 Complex Exponential Expansion Function

To allow us to use any function for the initial data we can use a complex exponential as the expansion function. However we first need the orthogonality condition for

complex exponentials,

$$\int_0^{2\pi} e^{imx} e^{-inx} dx = \begin{cases} 2\pi & \text{if } m = n \\ 0 & \text{if } m \neq n. \end{cases}$$

This means that our expansion functions are now $\varphi_k(x) = e^{ikx}$ and $\varphi_l(x) = e^{-ilx}$, using the definition Eq. (3.15) the mass and stiffness matrices are now,

$$M_{kl} = \int_0^{2\pi} e^{ikx} e^{-ilx} dx$$

and

$$D_{kl} = \int_0^{2\pi} (ik)^\alpha e^{ikx} e^{-ilx} dx.$$

The orthogonality condition means that both matrices are diagonal. Due to this and because it allows any initial data it will be the preferred choice of expansion function. However using definition Eq. (3.15) produces a result that diffuses in a left direction. We need to change this definition so it creates diffusion in a right direction. These can then be halved and summed together. To find this we take the derivative over $-x$ this idea comes from the definitions for fractional derivatives in which they are either defined as $\frac{d^\alpha f(x)}{dx^\alpha}$ or $\frac{d^\alpha f(x)}{d(-x)^\alpha}$. This gives our right sided fractional derivative for an exponential function as,

$$\frac{d^\alpha}{d(-x)^\alpha} e^{\lambda x} = (-\lambda)^\alpha e^{\lambda x} \quad (5.5)$$

Using both (3.15) and (5.5) gives the stiffness matrix as,

$$D_{kl} = \int_0^{2\pi} \left(\frac{(ik)^\alpha}{2} e^{ikx} e^{-ilx} + \frac{(-ik)^\alpha}{2} e^{ikx} e^{-ilx} \right) dx.$$

This causes a problem when $\alpha = 1$ as the values cancel out, however we also find that $\alpha = 1$ for cosine expansion functions does not produce a result. Since $\alpha = 1$ is advection and not diffusion we are not interested in this case. However, it does mean that the schemes we have developed using spectral methods are not as general as the finite difference methods and perhaps that our choice of expansion

function is not the best choice.

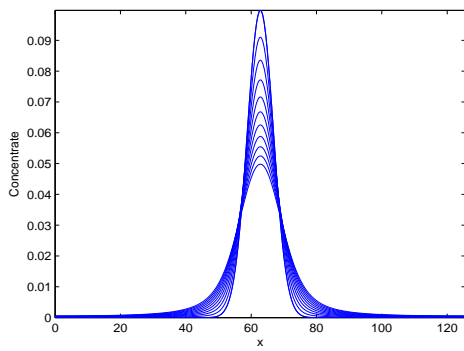
On the positive side we also find that the complex exponential case is valid on any domain.

5.3 Results and Comparison with Finite Difference Scheme

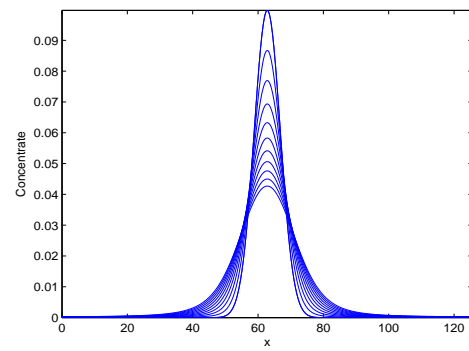
To look at a range of results and compare to our finite difference scheme we shall use the spectral method that uses complex exponential expansion functions. This is because it allows the diffusivity matrix to be diagonal and therefore reduces the computational time.

One problem with our method is that it uses periodic boundary conditions, so when the diffusion reaches the boundary it treats the value differently to the finite difference scheme. For this reason we will only compare results over a large domain so there is no interaction with the boundary.

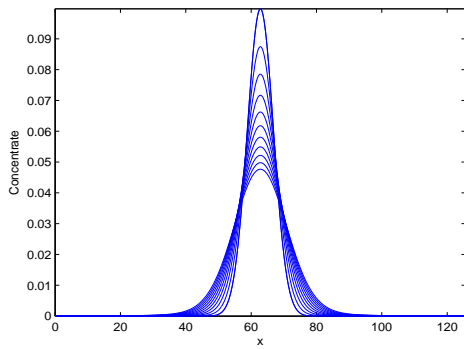
As with our finite difference scheme our initial data is Gaussian with a mean of 20π and standard deviation of four defined on $0 < x < 40\pi$. We use the same value of α as in the finite difference method with a final time of 20 seconds and output every two seconds. The results we obtain are very similar, see Fig. 5.3.



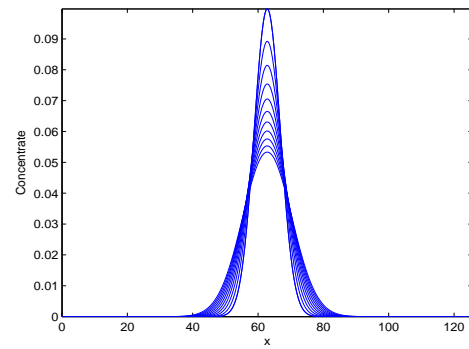
(a) $\alpha = 1.2$



(b) $\alpha = 1.5$



(c) $\alpha = 1.8$



(d) $\alpha = 2$

Figure 5.3: Fractional diffusion using a spectral method with complex exponential expansion functions

We then evaluate the standard deviation at various times and calculate its evolution see Fig. 5.4 this gives a very similar result to that displayed in Fig. 4.10.

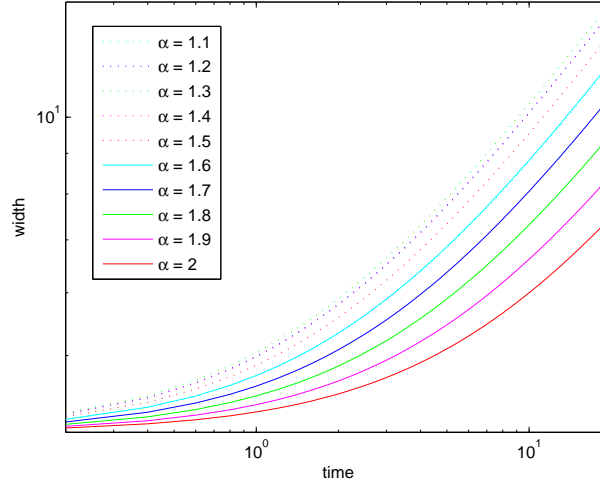
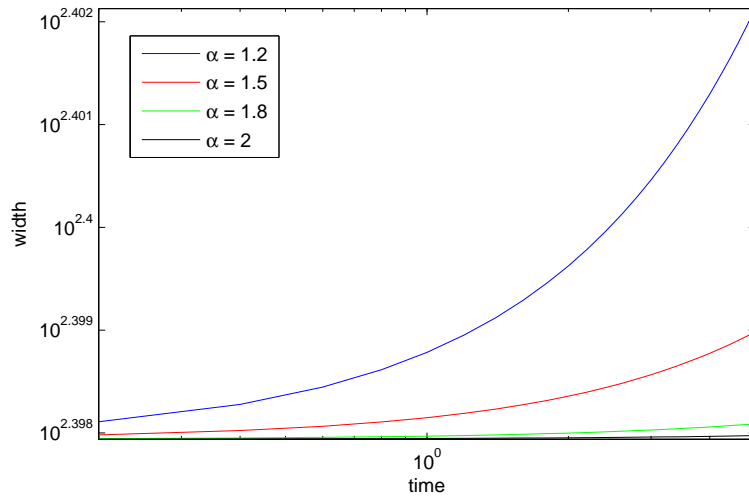


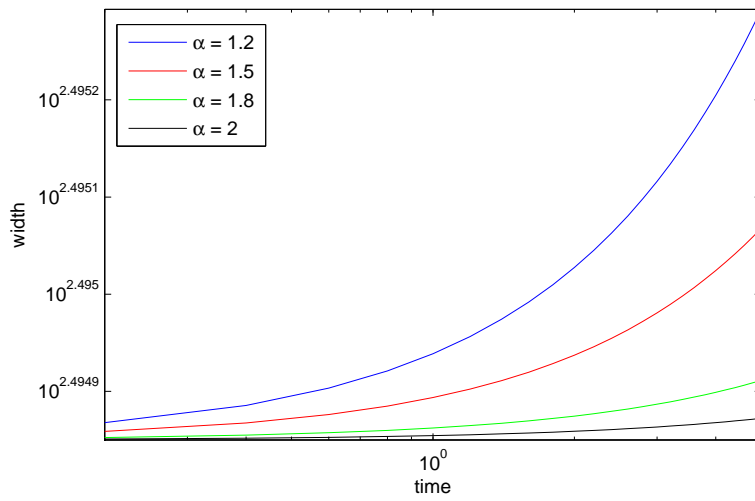
Figure 5.4: Width of diffusing plume plotted on loglog scale for spectral method

The main difference is for the small values of α . If we increase the size of the domain to 2500π and shorten the final time to 5 second to reduce the run time of the program as 2500π is a large domain, we can compare the widths of the concentration plumes for both methods Fig. 5.5 shows the results.

We notice that the scales are different but the slopes are similar. It appears that the spectral method produces results closer to what we expect sooner than the finite difference method. Perhaps this is due to the accuracy of the methods or because of the definitions for fractional derivatives used in each case. However to determine the cause this will require further investigation which will also help in determining the suitability of the spectral method. These results were produced without viewing the diffusion pattern and therefore further investigation is required in this area.



(a) Spectral method



(b) Finite difference method

Figure 5.5: Comparison of Plume Widths

Chapter 6

Conclusions and Future Work

6.1 Fractional Diffusion

We have determined that Levy distributions are a solution to the fractional diffusing equation, these Levy distributions have thicker tails meaning that the probability of particles jumping further is increased. Meaning that the fractional diffusion equation presents a valid alternative model to modelling diffusion in flows which have large variations in the velocity field.

Using fractional diffusion to model certain diffusion processes instead of the second of diffusion equation allows us to have greater control of the over the speed and spread of the diffusion. It means that the value of α can be chosen so it fits the diffusion pattern for any particular physical flow. In the paper by Benson [2] the values of K_α and α so the model fits real life results.

We have seen that it is easy to use fractional diffusion to model diffusion in a particular direction and at different rates. The control we have over the direction and rate of the diffusion is perhaps most noticeable in the two dimensional case. Here we have seen that there are so many different combinations of scheme we can use each giving very different results.

Further work can be done to fit the fractional diffusion equation to a real world example and assess the how well it fits the data over using the ordinary second order diffusion equation.

6.2 Finite Difference Method

The finite difference method is well defined and is the predominant method used in the literature. It is easy to implement and does not have any restrictions on initial data or domain size. We have been able to validate the finite difference method which gives us confidence that other results obtained from it are accurate.

The results obtained from using the central scheme show us different rates of dispersion for different α with the smaller α allowing a wider spread of contaminant particles. One area for further work is in determining a reason for the varying standard deviation for different sized domains. We have seen that the evolution of the standard deviation does not give what we expect. Indicating either that the method does not like interaction with the boundary or that it is simply better defined on a larger x domain.

This leads us on to another area for further work, the determination of valid boundary conditions. For advection, a first order derivative, we just require one boundary condition. For second order diffusion we require two. With fractional diffusion we are using a derivative with a real valued number between one and two. This could mean that we do not require two boundary conditions to solve this problem.

We have seen that the method is easy to expand into two dimensions and a wide variety of patterns of diffusion can be obtained. We have only looked at a few cases, further work could be done here to assess the suitability of different schemes for different initial data. An interesting area to look at has been the attempt to

modelling an advecting plume. Again only a few results have been produced here. Further investigation would allow us to determine whether using the fractional diffusion term allows a better fit for real life diffusing plumes such as smoke plumes from chimneys.

There is also future work in the determination of the relevance of the units in K_α . As mentioned we could solve using a dimensionless equation.

6.3 Spectral Method

The spectral method using complex exponentials produces promising results for the cases we have looked at in that they match up to the finite difference results well.

Further research needs to go into obtaining a method that will allow any boundary condition we define. Or how to allow the domain to be any size we require and not just multiples of π . It is possible that the boundary condition problem may be solved by taking different expansion functions. We would then have to determine what the fractional derivative of these expansion functions are. The reason for choosing the expansion functions detailed in Chapter 5 is that fractional derivatives for these functions have already been described in the literature. Once all these areas have been dealt with another area for future work is determining the stability regions and the order of accuracy.

The spectral method we have developed here should really be seen as an initial step forward and one that requires further research and validation.

Bibliography

- [1] D Benson, S Wheatcraft, M Meerschaert. *The fractional-order governing equation of Levy motion*, Water Resources Research 36 6 1413-1423, 2003
- [2] D Benson, S Wheatcraft, M Meerschaert. *Application of a fractional advection-dispersion equation*, Water Resources Research 36 6 1403-1412, 2000
- [3] C Canuto, M Y Hussaini, A Quarteroni, T A Zang. *Spectral Methods Fundamentals in Single Domains*, Scientific Computation Springer, 2006
- [4] J Crank. *The Mathematics of Diffusion*, Clarendon Press, 2nd Edition, 1975
- [5] B Cushman-Roisin. *Beyond Adolf Fick: A new model of turbulent dispersion*, Presentation, 2006
- [6] D Durran. *Numerical Methods for Wave Equations in Geophysical Fluid Dynamics*, Springer, 1999
- [7] Y Lin, C Xu. *Finite difference/spectral approximations for the time-fractional diffusion equation*, J. Comp. Phys. 225 1533-1552, 2007
- [8] M Meerschaert. *The Fractal Calculus Project*, Presentation, 2007
- [9] M Meerschaert, H P Scheffler, C Tadjeran. *Finite difference methods for two-dimensional fractional dispersion equation*, J. Comp. Phys. 211 249-261, 2006
- [10] M Meerschaert, C Tadjeran. *Finite difference approximations for fractional advection-dispersion flow equations*, J. Comp. and App. Math. 172 65-77, 2004

- [11] R Metzler, J Klafter. *The restaurant at the end of the random walk:Recent developments in the description of anomalous transport by fractional dynamics*, J. Phys. A 37 R161-R208, 2004
- [12] K Oldham, J Spanier. *The Fractional Calculus*, Academic Press, 1974
- [13] R Schumer, D Benson, M Meerschaert, S Wheatcraft. *Eulerian derivation of the fractional advection-dispersion equation*, J. Contam. Hydro. 48 69-88, 2001
- [14] D Sornette. *Critical Phenomena in Natural Sciences*, Springer, 2nd Edition, 2006
- [15] C Tadjeran, M Meerschaert, H P Scheffler. *A second-order accurate numerical approximation for the fractional diffusion equation*, J. Comp. Phys. 213 205-213, 2006
- [16] E Weisstein. *"Gamma Function."* *From MathWorld—A Wolfram Web Resource*, <http://mathworld.wolfram.com/GammaFunction.html>, 2008